Graduate Theses and Dissertations   Graduate School

3-24-2017

Sorption of Benzene, Dichloroethane, Chloroform and Dichloromethane by Polyethylene Glycol, Polycaprolactone and Their Copolymers at 298.15 K Using a Quartz Crystal Microbalance

Abhijeet Radhakrishna Iyer
University of South Florida, abhijeetiyer@mail.usf.edu

Follow this and additional works at: http://scholarcommons.usf.edu/etd

Part of the Chemical Engineering Commons

Sorption of Benzene, Dichloroethane, Chloroform and Dichloromethane by Polyethylene Glycol,

Polycaprolactone and Their Copolymers at 298.15 K Using a Quartz Crystal Microbalance

by

Abhijeet Iyer

A thesis submitted in partial fulfillment
of the requirements for the degree of
Master of Science in Materials Science and Engineering
Department of Chemical and Biomedical Engineering
College of Engineering
University of South Florida

Co-Major Professor: Venkat Bhethanabotla, Ph.D.
Co-Major Professor: Scott Campbell, Ph.D.
John Kuhn, Ph.D.

Date of Approval:
March 13, 2017

Keywords: organic vapor sensing, piezoelectric, activity, absorption, adsorption

DEDICATION

This thesis is dedicated to my parents, brother, and friends.

ACKNOWLEDGMENTS

I would like to express my sincere gratitude to my Co-major professors Dr. Venkat Bhethanabotla and Dr. Scott Campbell for giving me the opportunity to work on this thesis and for their continuous support and encouragement throughout the journey. I would like to thank Jonathan Samuelson for his technical help regarding the equipment setup, procedure and, troubleshooting. Finally, thanks to my family and friends for the constant support. Finally, I would whole heartedly thank Catherine Burton, Academic Program Specialist, for her guidance through the thesis formatting process.

TABLE OF CONTENTS

LIST OF TABLES

LIST OF FIGURES

ABSTRACT

Quartz crystal microbalances (QCM) are acoustic wave sensor systems which are used majorly for vapor and liquid sensing. QCM come under the category of thickness shear mode (TSM) sensors. There are several methods to study organic vapor sensing; the QCM method is the one that offers the highest sensitivity and generates the most data. Solubilities of benzene, dichloroethane, chloroform and dichloromethane in polyethylene glycol (PEG), polycaprolactone (PCL), and several di-block PEG/PCL copolymers at 298.15 K are reported. There are literature data available for most of the solvents in the homopolymers PEG and PCL but no literature data is available for the copolymers PEG (5000)/ PCL (1000), PEG (5000)/ PCL (5000) and PEG (1000)/ PCL (5000). Activity vs. weight fraction data was collected using a quartz crystal microbalance and are adequately represented by the Flory-Huggins model within experimental error. The data were reported using a QCM in a newly designed flow system constructed in the lab. The working apparatus consisted of a computer loaded with LabVIEW software for data selection, a quartz crystal cell, four bubblers for solvents, a phase lock oscillator, a frequency counter, and a temperature controlled vapor dilution system.

In this thesis, the proof for a working model of the QCM apparatus was reported through a test-case. The test case consists of a study that details the solubility of the polyisobutylene (PIB) polymer in benzene at 298.15 K which was then compared to previous work published in the literature.

CHAPTER 1: INTRODUCTION

1.1 Motivation

The QCM technique for thin film study was first introduced by King[1] is one of the oldest and most sensitive sensor systems. The comparison between experimental results and Masouka et al[2] literature data prove that the QCM technique used in the lab works well. To study the sorption process using the QCM technique, we choose two specific polymers, Polycaprolactone and Polyethylene Glycol. This is because, Polycaprolactone is the leading biodegradable compound approved by the Federal Drug Administration (FDA) for drug delivery systems, implants, adhesion barriers, and tissue engineering[3]. The rate at which polycaprolactones degrades is slow (3-4 years) due to its strong crystalline nature though it can be improved significantly by copolymerization with PEG[4]. The study of these polymer-solvent interactions is especially of interest to both academic and industry research given the wide range of applications of polymers and the sparse polymer property data that exists in literature to date. The study of thermodynamic parameters of these polymer-solvent interactions also helps make question and analyze the various existing thermodynamic models which will be discussed in the results and discussion section.

1.2 Background

Sorption usually refers to both phenomenon adsorption and absorption. This thesis studies the sorption of four solvents in five polymer systems. The sorption study was done using

the Quartz Crystal Microbalance which was modified in the laboratory by previous researchers. Previously reported results from our laboratory were obtained using a Quartz Crystal Microbalance in a static apparatus[5-8] but for this experimentation, a newly modified/designed flow system was constructed and used. The solubilities of benzene, dichloroethane, chloroform, and dichloromethane in the homopolymers polycaprolactone (PCL) and polyethylene glycol (PEG), as well as three di-block (PEG/PCL) copolymers at 298.15 K was presented. The copolymers are PEG (5000)/PCL (1000), PEG (5000)/PCL (5000), and PEG (1000)/PCL (5000), where the number in the parentheses represents the molecular weight of that segment of the polymer.

Polycaprolactone $(C_6 H_{10} O_2)_n$, a semi-crystalline polymer with a glass transition temperature of -60°C[9] and a melting point of around 59-64°C[9] is one of the prominent biodegradable polymers used in the 1970s-1980s for drug delivery and other biomaterial systems. But it was later forgotten due to its longer degradation time of 3-4 years, and intracellular resorption pathways[3]. Recent use of polycaprolactones as a copolymer with Polyethylene Glycol helped reduce its degradability by decreasing the crystallinity of the polymer due its high biocompatibility and hydrophilicity making it a favorable polymer for tissue engineering, biomaterials, and drug delivery systems[4]. The rheological and viscoelastic properties of PCL like low melting point, blend-compatibility with other polymers (PEG) makes it a favorable choice for biomedical applications[10]. There are various other polymers like Polylactic acid which can be copolymerized with PCL to form a favorable biodegradable polymer but the advantage of choosing PEG over others is due to the ease of synthesis of PCL with PEG by direct copolycondensation. Polyethylene Glycol having the glass transition temperature as same as Polycaprolactone is also an added advantage for copolymerization.

Polyethylene Glycol (PEG) which is also known as polyethylene oxide (PEO) based on its application is $H-(O-CH_2- CH_2)_n-OH$. It is prepared by the polymerization of ethylene oxide and finds extensive use in the industry and biomedical field. PEG is mostly soluble in all solvents like water, benzene, dichloromethane and is insoluble in hexane and diethyl ether and due to its biocompatibility nature; it is coupled with other hydrophobic polymers to produce non-ionic surfactants[11].

Caprolactones, as mentioned above, can be used extensively in the biomedical field but this is only possible when it is copolymerized with PEG to form diblock copolymers. The three diblock copolymers used here are PEG (1000)/ PCL (5000), PEG (5000)/ PCL (5000) and, PEG (5000)/ PCL (1000) with molecular weights mentioned in the parenthesis. The lower the molecular weight of the diblock copolymer, the easier it is to be tolerated inside the human body. These diblock copolymers are amphiphilic in nature i.e. they are both hydrophilic and lipophilic and thus act as polymersomes which form tiny spheres and further store the drug solution inside.

1.3 Quartz Crystal Microbalance

The piezoelectric effect is the ability of material to produce electric charges in response to mechanical stress is seen in quartz crystals. When the quartz crystals are AT-cut and some mechanical pressure is applied on the surface, it induces oscillations at a certain frequency. This resonant frequency is related to the mass of the crystal. Usually for any type of acoustic wave sensor, there is change in a physical quantity due to change in frequency, here it is mass. Sauerbrey[12] gave the relationship between resonance frequency shift (Δf) and the difference in mass of crystal (Δm) by the equation

$$\Delta f = -C_f \Delta m \quad (1)$$

where Δf is the change in frequency, C_f is the sensitivity factor and Δm is the change in mass/area

The Sauerbrey equation holds true only for gas-phase and is not applicable for liquid-phase measurements because of various liquid properties like viscosity and density impact the QCM[13]. The QCM sensor used in the experiment was a 5 MHz quartz crystal which was mounted by gold electrodes on both the sides. There are various methods of measuring thin films properties like surface plasmon resonance spectroscopy, ellipsometry but they have the disadvantage of restricted environment, large sample preparation time which the QCM overcomes. QCMs come under the category of piezoelectric thickness-shear-mode resonators which work on the basic principle of the relationship between resonant frequency and mass of rigid layers on the surface of the crystal. Nowadays QCM is used in various fields as mass detectors like in bio sensing, surface-molecule studies, gas detection, electrochemistry and environmental monitoring. QCM comes under the category of acoustic wave sensors.

Acoustic wave sensors work on the basic principle of change in resonant frequency resulting in a change in respective physical quantity like mass. In the case of QCM, the resulting change in resonant frequency corresponds to mass being measured. QCM are known to be one of the oldest, effective and sensitive acoustic wave sensors. They use a piezoelectric material which produces electrical output for a mechanical input to make this happen. QCM devices usually operate between 5-30 MHz but in this experiment, the 5 MHz crystal was used due to its higher sensitivity to polymer films[14]. At higher frequencies, the QCM are fragile. QCM's are also temperature dependent; they work well only in a proper range of temperatures. The 5MHz crystal work well at the room temperature. It was considered to have better sensitivity and temperature control as compared to the 10 MHz crystals used for similar experiments before.

1.4 Previous Work

Activity-weight fraction data for benzene in polyethylene glycol have been reported by Panayiotou and Veera[15] at 365 K for benzene weight fractions ranging from 0.06 to 0.47. Hao et al[16]. reported data for polyethylene glycol at 297.5 K for benzene weight fractions between 0.86 and 0.98 as well as at 333.15 K for chloroform in polycaprolactone at chloroform weight fractions in the range of 0.08-0.62. Booth et al.[17] reported data for chloroform sorption in polyethylene glycol with weight fractions ranging from 0.029 to 0.811; the data exhibited a marked inflection consistent with phase separation. There are no data reported for the PEG/PCL copolymers in the literature.

1.5 Thesis Outline

The thesis consists of five chapters. Chapter 1 talks about the motivation behind the thesis, background information about the experiment, and previous work done in this field. Chapter 2 discusses the thermodynamics of polymer solutions which includes Vapor Liquid Equilibrium and the Flory-Huggins model used for obtaining various results. Chapter 3 includes the materials used for the experiment, experimental procedure, QCM design and the apparatus design. The results and discussion are included in Chapter 4 followed by future work and conclusion in Chapter 5. Appendix A has some additional information about frequency-time curves for the sorption process and metadata file collected by the LabView software.

CHAPTER 2: THERMODYNAMICS

2.1 Introduction

Chapter 2 talks about the thermodynamic models and vapor-liquid equilibrium calculations for the polymer-solvent system. Solvent activities are derived in section 2.2 followed by Flory-Huggins model in section 2.3.

2.2 Vapor-Liquid Equilibrium

The term activity refers to the ratio of fugacity of specie to its fugacity at standard state. It is a dimensionless number. The value of activity is temperature, pressure and composition dependent. Here, we show how the activity a_1 of solvent 1 in the polymer phase is obtained from experimental parameters. We begin by equating the fugacity of the solvent in vapor and polymer phases:

$$f_1^{vapor} = f_1^{solution} \quad (2)$$

where,

f_1^{vapor} is the fugacity of the solvent in the vapor phase.

$f_1^{solution}$ is the fugacity of the solvent in the polymer phase.

Expressing the vapor phase fugacity in terms of fugacity coefficient and the liquid phase fugacity in terms of the activity coefficient yields:

$$\emptyset_1 y_1 P = \gamma_1 x_1 P_1^{sat} \quad (3)$$

where $\emptyset_1$ is the fugacity coefficient, y_1 is the mole fraction of the solvent in the vapor passing

over the polymer, P is the total pressure of the system, P_1^{sat} is the saturated vapor pressure at cell temperature T, and x_1 is the mole fraction of the specie 1 in the polymeric phase.

The fugacity coefficient is given by,

$$\emptyset_1 = \exp\left[\frac{P}{RT}\left(B_{11} + y_3^2(2 B_{13} - B_{11} - B_{33})\right)\right] \quad (4)$$

where B_{11} is the second virial coefficient of the pure solvent, B_{33} is the second virial coefficient of nitrogen, and B_{13} is the second virial cross coefficient. All of them are calculated using

$$B_{ij} = \frac{RT_c}{P_c}[f^0(T_R) + \omega f^1(T_R)] \quad (5)$$

where ω is the Pitzer's accentric factor, T_c, P_c are critical temperature and pressure respectively, T_R is the reduced temperature. $f^0 \ and \ f^1$ are given by the Tsonopolous[18] equation:

$$f^{(0)}(T_R) = 0.1445 - \frac{0.330}{T_R} - \frac{0.1358}{T_R^2} - \frac{0.0121}{T_R^3} \quad (6)$$

$$f^{(1)}(T_R) = 0.073 - \frac{0.46}{T_R} - \frac{0.5}{T_R^2} - \frac{0.097}{T_R^3} - \frac{0.0073}{T_R^3} \quad (7)$$

Calculation of B_{13} requires a binary interaction coefficient. The binary interaction coefficient for benzene + nitrogen was taken from Meng and Duan[19]. A binary interaction coefficient for nitrogen + chloroform was extracted from second virial cross coefficient data in Dymond and Smith[20] and was also applied to nitrogen + dichloroethane and nitrogen + dichloromethane. Substituting for $\emptyset_1$ in equation (3) using equation (4) and noting that $a_1 = \gamma_1 x_1$ the solvent activity is:

$$a_1 = \frac{y_1 P}{P_1^s(T)} \exp\left[\frac{P}{RT}\left[B_{11} + \left(1 - y_1\right)^2(2B_{13} - B_{11} - B_{33})\right]\right] \quad (8)$$

As will be seen in the next chapter, solvent vapor is created by passing a stream of nitrogen gas through a solvent storage unit, where liquid solvent vaporizes until equilibrating

with the liquid solvent. The mole fraction y_{1B} of solvent in the gas stream leaving the solvent

storage unit can be computed from equation (3) by applying the right side to the liquid solvent in

the solvent storage unit and the left side to the vapor exiting the storage unit. In this event, $\gamma_1 = 1$, $x_1 = 1$ and

$$y_{1B} = \frac{P_1^{sat}}{P\emptyset_1}(T',P) \quad (9)$$

where the functional notation indicates that the quantities on the right side of the equation are

evaluated at the temperature T' of the solvent storage unit and pressure P.

Vapor pressures P_1^S at both temperatures T and T' were obtained using the Antoine

equation:

$$\log_{10} P_1^s(bars) = A - \frac{B}{T'(K)+C} \quad (10)$$

where T' represents either the solvent storage unit temperature or the cell equilibrium

temperature T. values for the constants[21] A, B, C are given in Table 2-1.

Table 2.1 Values of coefficients used for calculating solvent vapor pressures

Antoine parameter	Benzene	Dichloroethane	Chloroform	Dichloromethane
A	4.01814	4.58518	4.20772	4.52691
B	1203.835	1521.789	1233.129	1327.016
C	-53.226	-24.67	-40.953	-20.474

2.3 Flory-Huggins Model

For studying the thermodynamics of polymer solutions, the Flory-Huggins model

investigated by Paul Flory and Maurice Huggins was used. The data were correlated by fitting

the experimental solvent activity - solvent weight fraction data to the Flory-Huggins model:

$$\frac{NG^E}{RT} = N_1 \ln\frac{\emptyset_1}{X_1} + N_2 \ln\frac{\emptyset_2}{X_2} + \chi\emptyset_1\emptyset_2(N_1 + rN_2) \quad (11)$$

8

where X_i is mole fraction (1 = solvent, 2 = polymer), $\emptyset_i$ is volume fraction, $r = V_2/V_1$ is the ratio of molar volumes, N_i is number of moles, and χ is used here as an adjustable parameter. The volume fractions of each component i are given by

$$\emptyset_i = \frac{V_i X_i}{\Sigma V_i X_i} \quad (12)$$

Molecular weights and molar volumes for the homopolymers, copolymers, and solvents are given in Table 2-2. Molar volumes of the homopolymers and solvents were calculated from known densities and molecular weights. For copolymers, specific volume was assumed to be a weight fraction average of the specific volumes of the homopolymers. The molar volume was then calculated from the specific volume by multiplying by the molecular weight of the copolymer. From equation (11), the expression for solvent activity a_1 can be derived:

$$\ln a_1 = \ln\emptyset_1 + \left(1 - \frac{1}{r}\right)\emptyset_2 + \chi\emptyset_2{}^2 \quad (13)$$

Values of χ were obtained by minimizing the sum of the squares of the differences between experimental and calculated activities and are given for each solvent-polymer system in Table, along with the average difference between experimental weight fraction and that calculated from the Flory-Huggins model. The model represents experimental weight fractions to within an average between 0.001 and 0.004.

Table 2.2 Molar mass (M) and molar volume (V) of the solvents and polymers

Species	M/g · mol^{-1}	V/cm^3 · mol^{-1}
Solvents		
Benzene	78.11	92.41
Dichloroethane	98.95	78.97
Chloroform	119.37	80.17
Dichloromethane	84.93	64.02
Polymers		
Polycaprolactone (PCL)	14000	12216.40
PEG (1000)/ PCL (5000)	6000	5195.40
PEG (5000)/ PCL (5000)	10000	8530
PEG (5000)/ PCL (1000)	6000	5038.80
Polyethylene Glycol (PEG)	2000	1666.67

9

CHAPTER 3: EXPERIMENTAL APPARATUS

3.1 Materials

PEG and PCL were obtained from Sigma-Aldrich with weight-average molecular weights of 2000 and 14000, respectively. PEG (5000)/PCL (5000), PEG (1000)/PCL (5000), and PEG (5000)/ PCL (1000) di-block copolymers were obtained from Polysciences, Inc. Benzene, dichloromethane, chloroform and dichloroethane were obtained from Sigma-Aldrich with 99.9% purity and were used with no further purification.

The 5 MHz quartz crystals (1-inch diameter, 0.013 inches thick, AT-cut) utilized in this study were supplied by Phillip Technologies (Greenville, South Carolina) and exhibited good piezoelectric and mechanical properties. The crystals were well-polished and had gold-coated electrodes. Their operating range was 4.976-5.020 MHz with resistances of approximately 10 ohms. The research crystals have an advantage of being used with any type of crystal holder and for thin film or liquid deposition. The quartz crystals which were ordered from Phillip technologies have extreme mechanical, electrical and piezoelectric properties allowing for improved stability by reducing the changes in frequency. The crystals are wrapped around with gold electrodes on both the sides to create a hydrophilic surface for film or liquid coating. Earlier experimentation done in this field used a 10 MHz crystal, but the 5 MHz crystal used in this experiment are considered to have better sensitivity. The 5 MHz crystal used here had a crystal thickness of 0.013 inch. The resistances of the 5MHz crystal were tested to be between 10-20 ohms and viscoelastic effects were seen for resistances above this range. Few readings for which

the resistances were high, were considered inaccurate. The following table shows the basic features of the gold-plated quartz crystal used in the experimentation.

Table 3.1 Properties of quartz crystal

Frequency	5 MHz
Frequency Range	4.976-5.020 MHz
Resistance	~10 ohms
Diameter of crystal	1 inch
Electrode diameter	0.5 inch
Crystal thickness	0.013 inch
Surface roughness	50 A
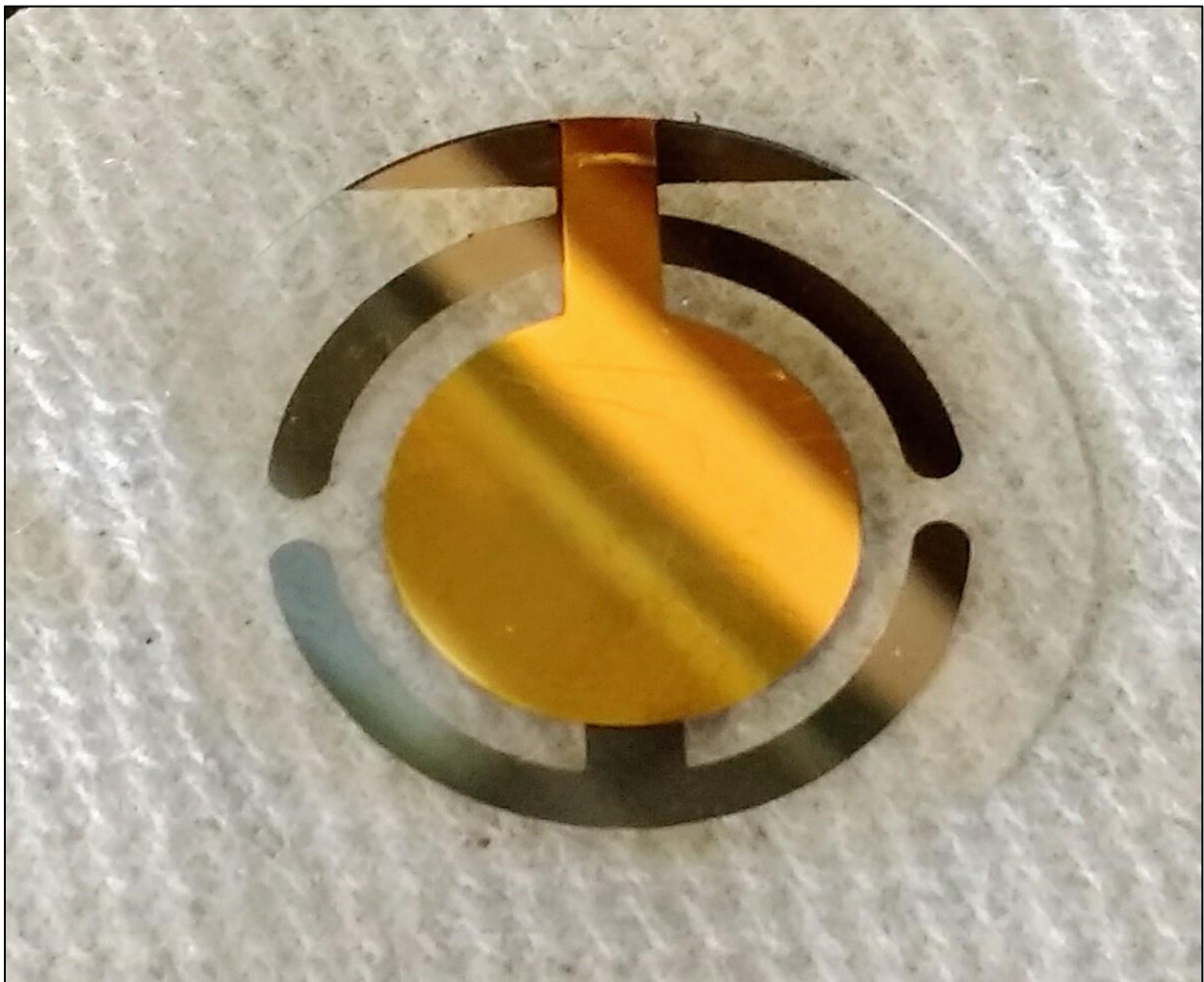
Figure 3.1 Quartz crystal used in the experiments (front)

Figure 3.2 Quartz crystal used in the experiments (rear)

3.2 Apparatus Design

The working apparatus consisted of a stream of solvent vapor diluted with nitrogen to arbitrary concentration passing over a QCM oscillated to its resonant frequency. The experiment and data collection were automated by a custom LabView script running on a computer connected to the main apparatus. The diagram for experimental apparatus is shown in Figure 1.

A size-300 tank (T1) of prepurified-grade nitrogen gas fed two MKS1179A mass-flow controllers (MFC1 and 2), which were computer-controlled to produce flows ranging from (0 to 100) sccm in increments of 10 sccm that together sum to 100 sccm to maintain a constant flow. The MFC1 flow was routed through one of four impingers (I1 - 4) by two banks of normally-closed solenoids (FV1A - 4A and FV1B - 4B) which were activated by computer-controlled relays so that only one flow path was open at a given time. The nitrogen gas bubbled through a reservoir of solvent in each impinger and the equilibrated bubbler vapor stream was diluted by the MFC2 diluent flow; the impingers were meanwhile kept at a constant temperature by a NESLAB RTE 740 recirculating chiller (HX1). In this way, up to ten different isothermal concentrations of solvent vapor for four different solvents could be produced by automated software.

The vapor was routed through a cell containing a 5.00 MHz QCM oscillated to its resonant frequency via a PLO-10i phase-lock oscillator (Maxtek) and the frequency, measured by an HP5334B frequency counter, was logged via computer. The cell was kept at a constant temperature by another NESLAB RTE 17 recirculating chiller (HX2) which also preheated the vapor entering the cell via a separate heat exchanger (HX3). Frequency-time data were logged and a running list of the last fifty data points was stored; when the slope of the frequency vs. time regression line was within a 95% confidence interval of 0 and the standard deviation of the frequency data was less than 0.9 Hz, the system was at equilibrium and the average and standard deviation were reported. These data were then used to calculate weight fractions; if the Butterworth-van Dyke equivalent resistance was below 20 Ohms, the data were considered reliable in representing true weight fractions. The data set for all the experiment done here had the resistance values between 10-20 ohms, because above that value indicates viscoelasticity.
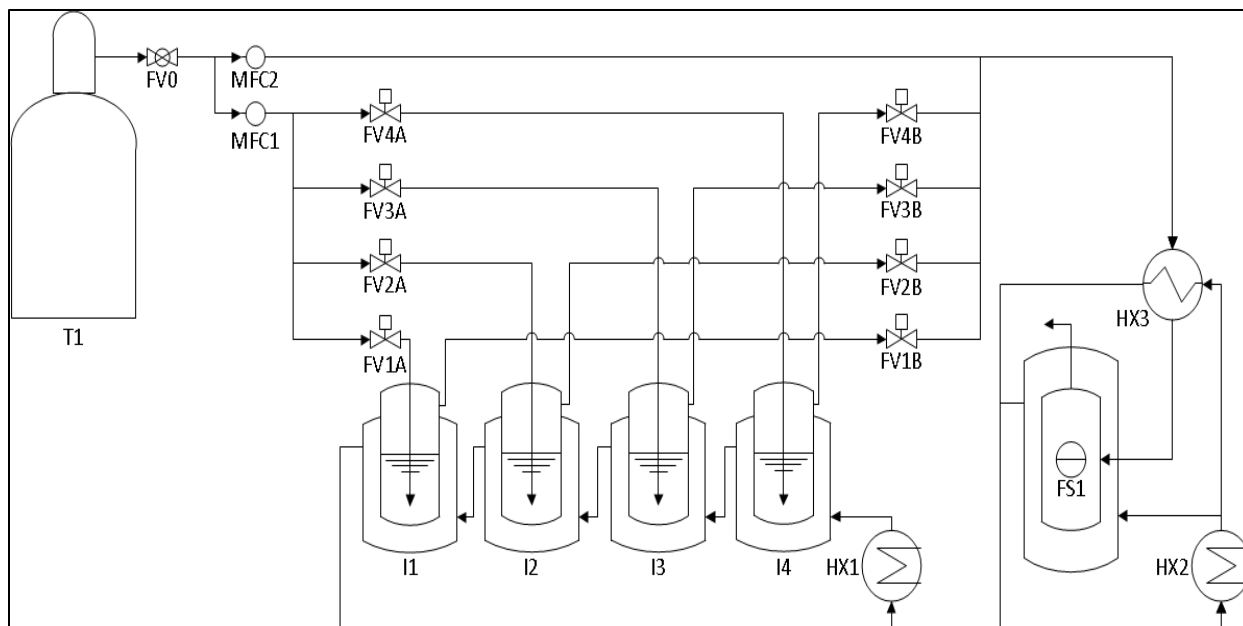
Figure 3.3 Schematic diagram of the quartz crystal microbalance apparatus
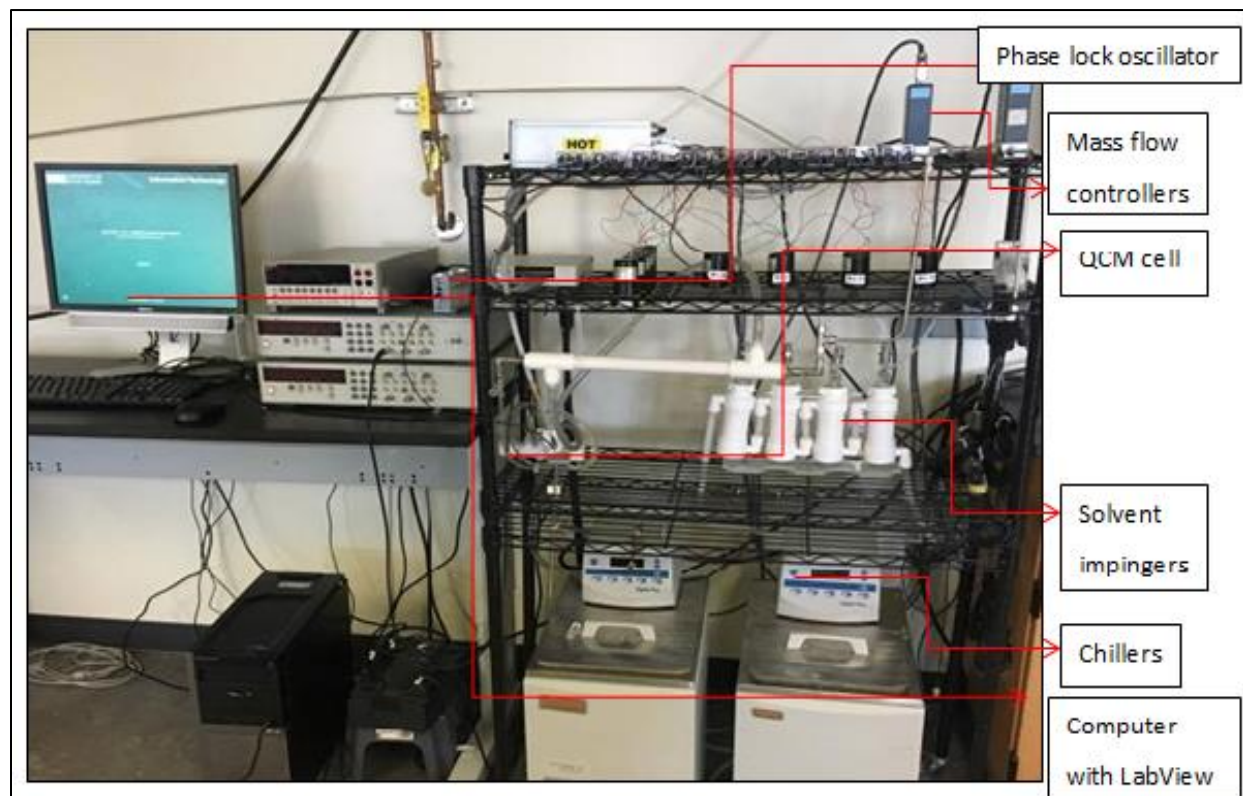
Figure 3.4 Experimental apparatus

3.3 QCM Design

The QCM was first designed by Sauerbrey to demonstrate the piezoelectric applications of the device towards change in the mass deposition on the surface of electrodes. QCM works on the basic principle of change in mass of the crystal due to changes in frequency which is given by the equation

$$\Delta f = -C_f \Delta m \quad (14)$$

where Δf is the change in frequency, C_f is the sensitivity factor and Δm is the change in mass/area

In general, QCM does not need calibration because of the linear sensitivity factor used in the above equation. The electrical working of the QCM is explained using the Butterworth van Dyke (BVD) model. The model helps predict the resonance, frequency shifts and losses of the crystal in use.
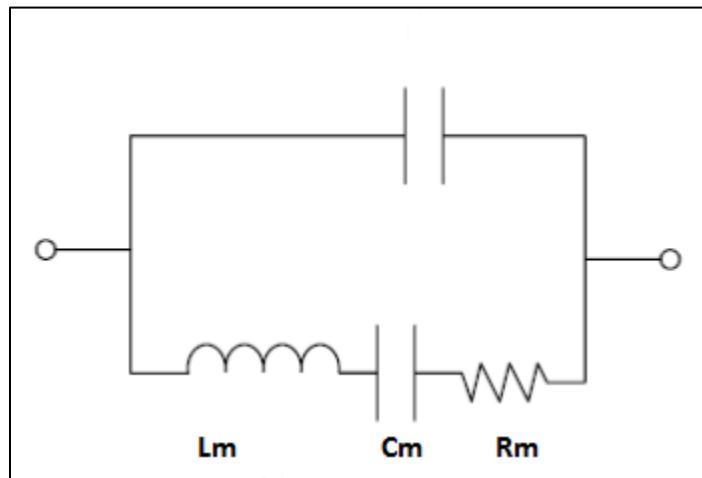
Figure 3.5 Butterworth-van Dyke model for QCM

The BVD model consists of a motional arm and static arm. The motional arm has the R_m (resistor), C_m (capacitor) and L_m (inductor) in series which is modified based on the mass loadings on the crystal. Each of these components correspond to dissipation or storage of

15

oscillation energy, for e.g. the resistor dissipates oscillation energy when the crystal meets other mediums, capacitor stores the energy which can be related to the elasticity of the crystal with the other medium and inductor is relevant to the initial oscillation of the crystal due to displacement of mass. For a 5MHz dry crystal of 1" diameter, the values of these components[22] are L_m= 30mH, R_m= 10 ohms and C_m= 33fF.
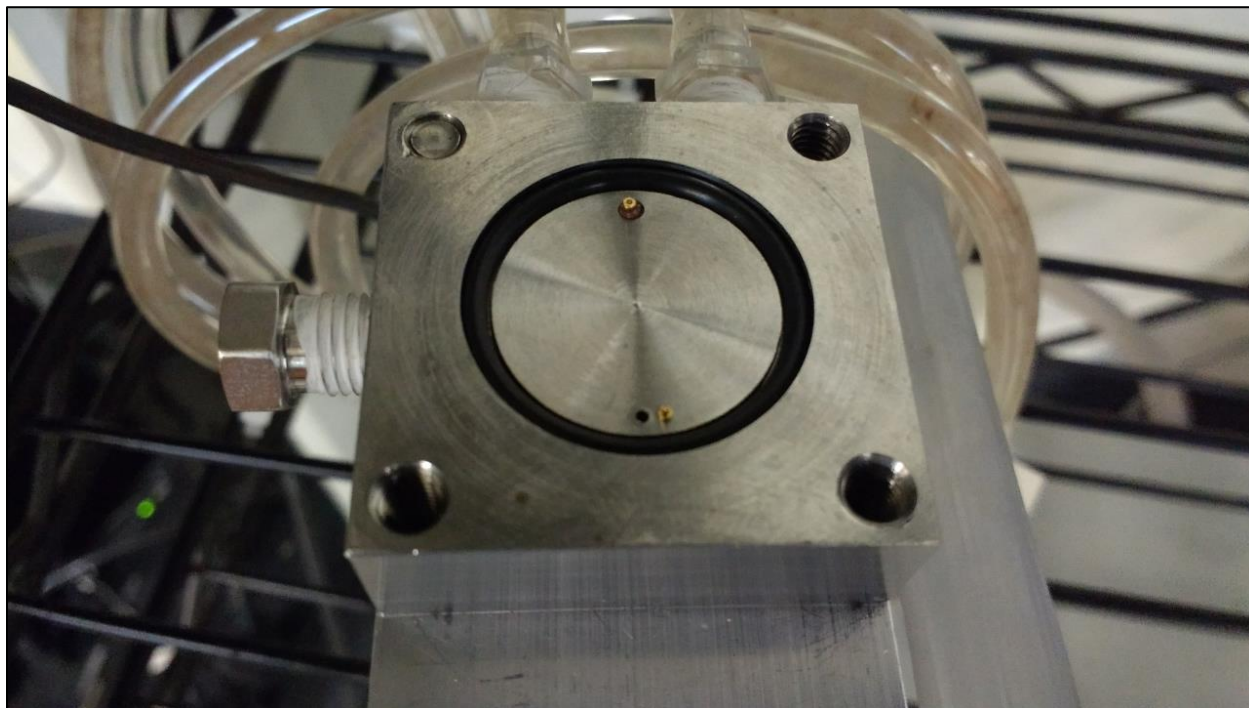
Figure 3.6 QCM cell

3.4 Procedure

The overall experimentation consists of three steps: polymer preparation, data collection, and cleaning. Polymer preparation involves selecting the appropriate solvent to make the polymer solution that then coats on the quartz crystal. A good solvent should not chemically alter the polymer, dissolve the polymer completely, become viscous when saturated and evaporate

16

quickly if not immediately. Toluene was the first choice for most polymer solutions except for the copolymer PEG (1000)/PCL (5000) which required chloroform. 10 mL of the solvent was added to 0.5 g of the polymer in a 20-mL vial and sonicated with heating for an hour to ensure proper mixing. Once the polymer solution was prepared, 300 uL of the solution was coated on the surface of the crystal using a spin coater. A good coating reads around 1000-5000 Hz frequency.

The data collection step includes using the LabView software to collect the weight fraction, resistance, frequency, and the standard deviation data for the run being done. The plasma cleaned crystal is placed in the cell and the frequency is supposed to change from 3.5 MHz to 5 MHz. The phase lock oscillator is adjusted to ensure the baseline frequency data and other data points are accurate. The nitrogen tank, MKS box, chillers, and the computer should be switched on to start collecting the data points. Firstly, the baseline frequency data point is collected by the LabView software followed by the data points for the coated crystal. The weight fractions, resistances, and propagated errors are found in the metadata file while the raw frequency-time data are found in the data file. This data help us analyze the sorption of the four solvents in the polymers by plotting the activity-weight fraction curve and the frequency-time curve.

The cleaning process involves step by step removal of the PEG/PCL coating on the quartz crystal. Firstly, the coated crystals are wrapped in a Kim-wipe and placed in the Soxhlet extractor which is mounted by a condenser. Dichloroethane solvent was used in the Soxhlet extractor flask as the choice of solvent to clean the PEG/PCL coatings. It takes roughly 6 hours for the cleaning process in the Soxhlet extractor. After the initial cleaning treatment, the wrapped crystals are sonicated and heated in a 250ml beaker of DI water and HCl for one hour.
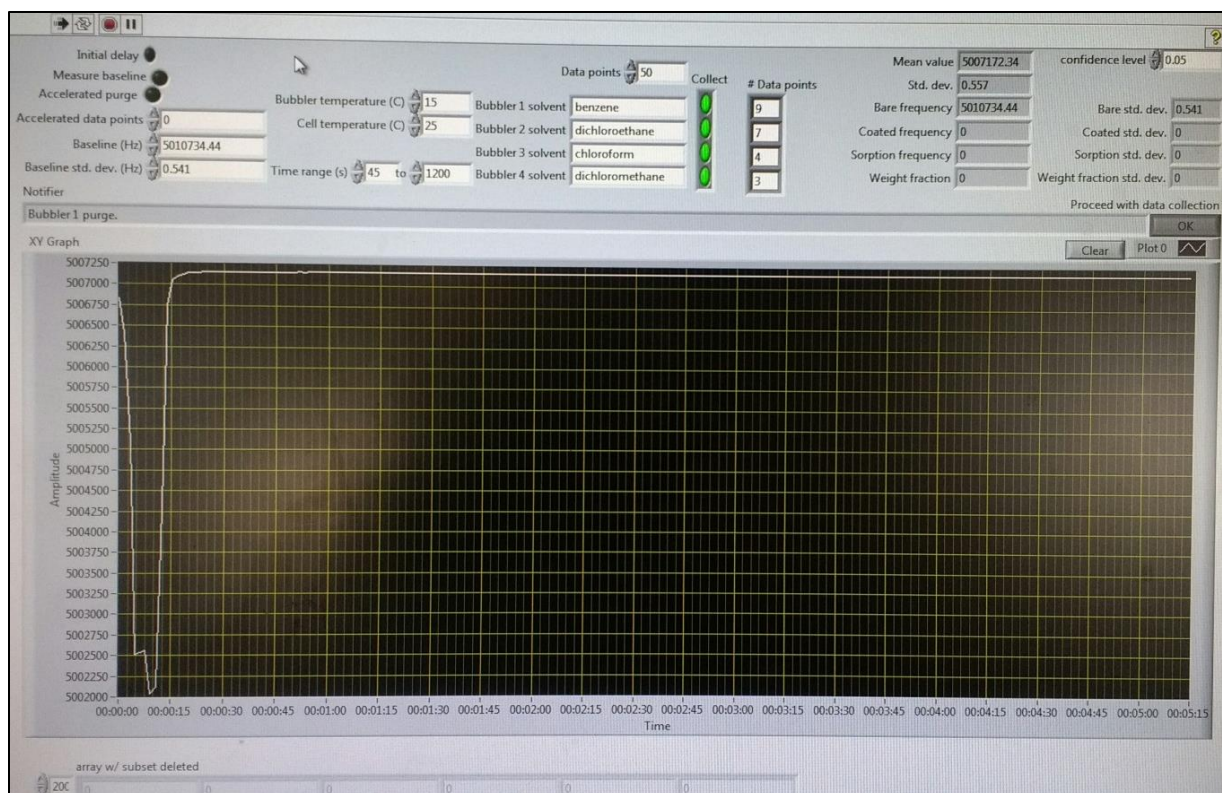
Figure 3.7 Screenshot of LabView software used

The crystals are dried off by blowing nitrogen over the crystals. The final step involves the crystals being plasma cleaned. A clean crystal should show roughly 5 MHz on the frequency counter. Crystals used in the experiment – both new and reused – were cleaned prior to spin-coating of the polymer or copolymer by means of Soxhlet extraction for six hours with dichloroethane followed by one hour of sonication in hydrochloric acid. The crystals were then rinsed clean with purified water and dried under a stream of nitrogen before plasma cleaning for 15 minutes on both sides. A polymer film was then applied to the clean crystals by means of spin-coating with a solution of the polymer in chloroform (for PEG (1000)/PCL (5000)) or toluene (for all others) to a frequency shift Δf_0 of 1000-5000 Hz between the uncoated and coated crystals. For each of the four solvents, the polymer was purged with nitrogen until the

frequency stabilized before applying gradually increasing concentrations of solvent vapor at constant flow. The frequency shift Δf between the purged crystal and the crystal with sorbed solvent was used in conjunction with Δf_0 to obtain the weight fraction w_1 via the Sauerbrey[9] equation as shown below.

$$w_1 = \frac{\Delta f}{\Delta f + \Delta f_0} \quad (15)$$

where Δf_0 is the frequency shift due to the mass of polymer film and Δf is the frequency shift due to the mass of sorbed solvent.

The mole fraction y_1 in equation (9) was obtained from:

$$y_1 = \frac{y_{1B} V_{31}}{V_{31} + (1 - y_{1B}) V_{32}} \quad (16)$$

where y_{1B} is the mole fraction of solvent in the gas stream leaving the impinger and V_{31} and V_{32} are the volumetric flow rates of nitrogen passing through mass flow controllers MFC1 and MFC2, respectively. They are mentioned below in Table 2-1. Mole fraction y_{1B} was obtained assuming the solvent vapor and nitrogen reach equilibrium in the impinger and requires a trial and error solution of:

$$y_{1B} = \frac{P_1^s(T')}{P} \frac{1}{\exp\left[\frac{P}{RT'}\left(B_{11} + (1 - y_{1B})^2 (2B_{13} - B_{11} - B_{33})\right)\right]} \quad (17)$$

where $P_1^S(T')$ is the solvent vapor pressure at the temperature T' of the impinger.

Equilibrium in the impingers was verified by gas chromatography for the solvents benzene and chloroform. Known masses of solvent were injected into a sealed container of nitrogen at atmospheric pressure and known temperature. The mole fraction y of the solvent was calculated and the relative percent area A of the solvent peak was obtained by injection into an

19

Agilent GC 7890A gas chromatograph. The calibration curve was linearized by plotting 1/y-1

versus (100-A)/A with coefficients of determination of 0.9995 or better. Vapor samples from the

apparatus during normal operation were collected and the relative percent areas were used to

calculate mole fractions which were then compared to values calculated by assuming equilibrium

was reached in the impingers. Results deviated by a %AARD of 2.6% for chloroform and 1.2%

for benzene. The assumption that equilibrium was achieved in the impingers was subsequently

used in all calculations.

Neglecting the effect of gas non-ideality in error estimation, the uncertainty σ_{a1} in

calculated solvent activity is given by:

$$\frac{\sigma_{a1}}{a_1} = \frac{d\ln P_s(T')}{dT'}\sigma_{T'} + \frac{d\ln P_s(T)}{dT}\sigma_T + \frac{\sigma_v}{V} \quad (18)$$

where σ_v is the uncertainty in volumetric flow rate V (= $V_{31}+V_{32}$), and σ_T and $\sigma_{T'}$ are

uncertainties in cell and impinger temperatures, respectively. The values for σ_T and $\sigma_{T'}$ are 0.01

and the uncertainty in volumetric flow rate is 1%. The values for deviation in temperature in the

recirculating chillers are derived from the company manual. Thus, uncertainties in activity are

less than 1.5%. The uncertainty σ_{w1} in weight fraction is given by:

$$\sigma w_1 = \frac{\frac{\sigma\Delta f}{\Delta f_0} + (\frac{w_1}{1-w_1})(\frac{\sigma\Delta f_0}{\Delta f_0})}{(1+\frac{w_1}{1-w_1})} \quad (19)$$

where $\sigma_{\Delta f}$ and $\sigma_{\Delta f0}$ are uncertainties in frequency shifts Δf and Δf_0. Resulting uncertainties in

weight fractions are 0.0006 or less. The reason why the uncertainties in weight fraction are low is

because the deviations in frequency are very low and that results in further uncertainty. The

Flory-Huggins model also calculates the deviations in weight fraction which will be discussed in

the later section.

Table 3.2 Volumetric flow rates of nitrogen passing through mass flow controllers MFC1 and

MFC2, respectively

V_{31}	V_{32}
10.2	87.8
20	78
30.6	67.8
40.6	58.8
50.4	48.5
60.3	38.2
70.9	29.8
81	19.2
90.9	9.6
102	0

Figure 3.8 Solutions of polymers prepared for the experiment

Table 3.3 Coating techniques of polymers

Coating	Coating Procedure	Solution
PCL	10,100 rpm for 10 minutes	0.5 g/ml in Toluene
PCL (5000)/ PEG (1000)	10,100 rpm for 10 minutes	0.5 g/ml in Chloroform
PCL (5000)/ PEG (5000)	10,100 rpm for 10 minutes	0.5 g/ml in Toluene
PCL (1000)/ PEG (5000)	10,100 rpm for 10 minutes	0.5 g/ml in Toluene
PEG	10,100 rpm for 10 minutes	0.5 g/ml in Toluene

Figure 3.9 Plasma cleaner used in the experiment to clean the crystal

Figure 3.10 Soxhlet extractor used in the experiment for cleaning process

Figure 3.11 Spin coater for the polymer coating on the cell

CHAPTER 4: RESULTS AND DISCUSSION

4.1 Results

The results section involves proof of the working model of the equipment used in this thesis. The proof consists the study of sorption of benzene in polyisobutylene (PIB) at 298.15 K and compared to previous literature[2]. Table 4.1 shows the weight fraction of benzene in PIB as collected using the present QCM apparatus and Figure 4.1 shows the comparison of experimental results to literature result.

Solvent weight fraction as a function of solvent activity for the four solvents in the copolymer system at 298.15 K are given in Tables 4-2, 4-3, 4- 4, and 4-5. As noted earlier, the software which controls the experiment can generate ten concentrations of each solvent.   Data for the lowest eight, five, and four are reported for dichloroethane, chloroform, and dichloromethane, respectively, as at higher solvent activities, a second phase with different properties formed. This will be discussed later; for all data reported in Tables 4-2 to 4-5, only a vapor phase and a single polymer phase are present at equilibrium.

Plots of solvent activity versus weight fraction for each solvent are shown in Figures 4-2 to 4-5. Close inspection of these figures reveals that, except for benzene, the variation of weight fraction with PCL/PEG ratio at constant activity is not monotonic. For the halogenated solvents, weight fractions at constant activity are lowest for PEG and increase with increasing PCL/PEG ratio, reaching a maximum for the PEG (1000)/PCL (5000) co-polymer, then decreasing slightly for the PCL homopolymer.

Table 4.1 Experimental data for weight fraction w_1 of benzene in PIB as a function of benzene

activity a_1

Activity (a_1)	Weight fraction (w_1)
0.069	0.010
0.134	0.020
0.203	0.031
0.264	0.042
0.327	0.054
0.390	0.067
0.445	0.081
0.507	0.097
0.563	0.114
0.618	0.132
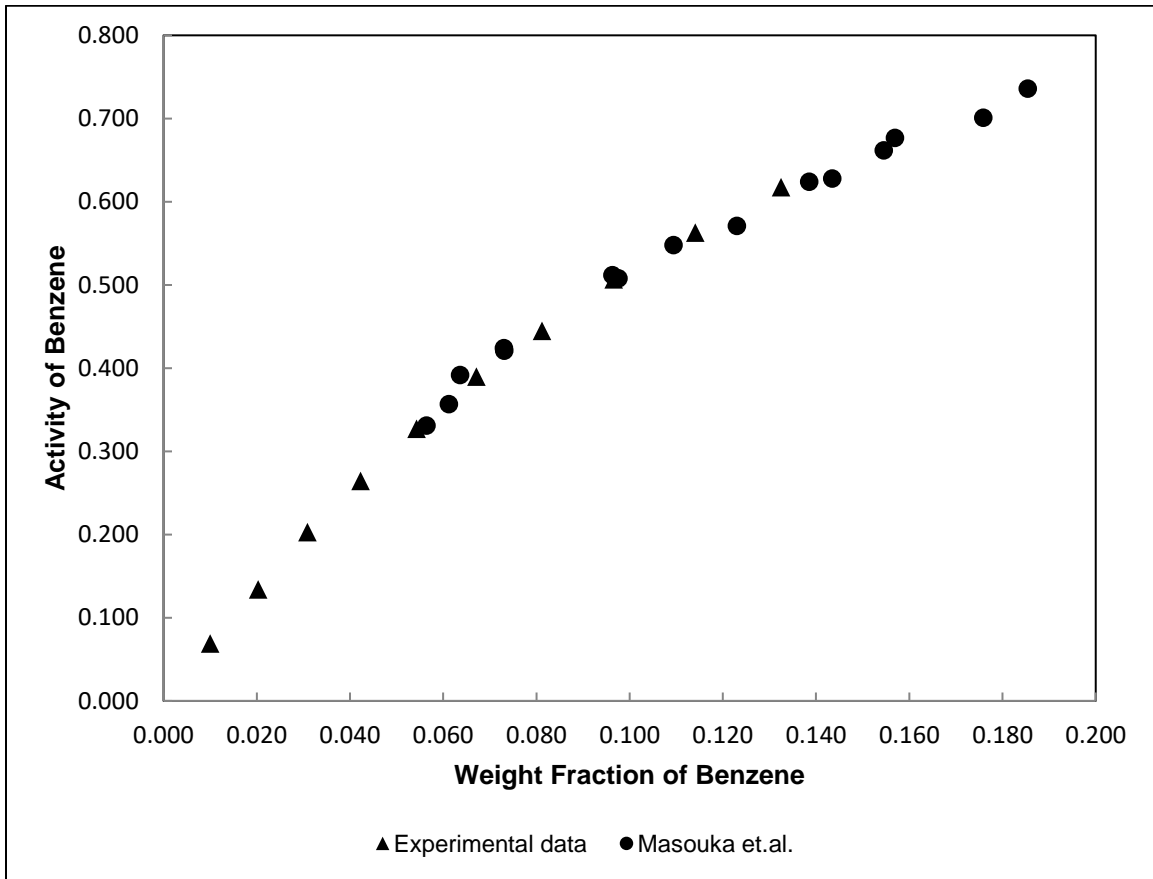
Figure 4.1 Activity versus weight fraction for benzene in PIB at 298.15 K

Table 4.2 Experimental data for weight fraction w_1 of benzene in PCL, PEG (1000)/ PCL (5000),

PEG (5000)/ PCL (5000), PEG (5000)/ PCL (1000), and PEG at 298.15 K as a function of

benzene activity a_1

Activity	w_1				
a_1	PCL	PEG (1000)/PCL (5000)	PEG (5000)/PCL (5000)	PEG (5000)/PCL (1000)	PEG
0.069	0.007	0.009	0.007	0.005	0.001
0.134	0.016	0.016	0.013	0.010	0.002
0.203	0.025	0.025	0.018	0.016	0.004
0.264	0.033	0.033	0.024	0.021	0.005
0.326	0.042	0.042	0.030	0.027	0.006
0.389	0.052	0.051	0.036	0.034	0.008
0.443	0.062	0.061	0.042	0.041	0.009
0.504	0.075	0.072	0.049	0.048	0.011
0.560	0.092	0.085	0.057	0.057	0.013
0.614	0.110	0.098	0.066	0.067	0.015

Table 4.3 Experimental data for weight fraction w_1 of DCE in PCL, PEG (1000)/ PCL (5000),

PEG (5000)/ PCL (5000), PEG (5000)/ PCL (1000), and PEG at 298.15 K as a function of DCE

activity a1

Activity	w_1				
a_1	PCL	PEG (1000)/PCL (5000)	PEG (5000)/PCL (5000)	PEG (5000)/PCL (1000)	PEG
0.068	0.014	0.017	0.013	0.010	0.003
0.133	0.029	0.034	0.026	0.021	0.006
0.201	0.043	0.051	0.037	0.031	0.009
0.262	0.059	0.067	0.048	0.042	0.012
0.325	0.074	0.084	0.059	0.054	0.016
0.387	0.092	0.101	0.073	0.067	0.020
0.442	0.112	0.119	0.090	0.082	0.024
0.504	0.134	0.138	0.120	0.101	-

Table 4.4 Experimental data for weight fraction w_1 of chloroform in PCL, PEG (1000)/ PCL (5000), PEG (5000)/ PCL (5000), PEG (5000)/ PCL (1000), and PEG at 298.15 K as a function of chloroform activity a_1

Activity	w_1				
a_1	PCL	PEG (1000)/PCL (5000)	PEG (5000)/PCL (5000)	PEG (5000)/PCL (1000)	PEG
0.079	0.038	0.044	0.033	0.028	0.008
0.152	0.073	0.085	0.062	0.055	0.016
0.227	0.108	0.121	0.091	0.082	0.025
0.292	0.143	0.154	0.126	0.112	0.038
0.357	0.193	0.199	-	-	-

Table 4.5 Experimental data for weight fraction w_1 of DCM in PCL, PEG (1000)/ PCL (5000), PEG (5000)/ PCL (5000), PEG (5000)/ PCL (1000), and PEG at 298.15 K as a function of DCM activity a_1

Activity	w_1				
a_1	PCL	PEG (1000)/PCL (5000)	PEG (5000)/PCL (5000)	PEG (5000)/PCL (1000)	PEG
0.104	0.031	0.039	0.034	0.024	0.008
0.192	0.061	0.072	0.064	0.046	0.016
0.276	0.092	0.101	0.098	0.069	0.025
0.345	0.123	0.128	-	0.097	-
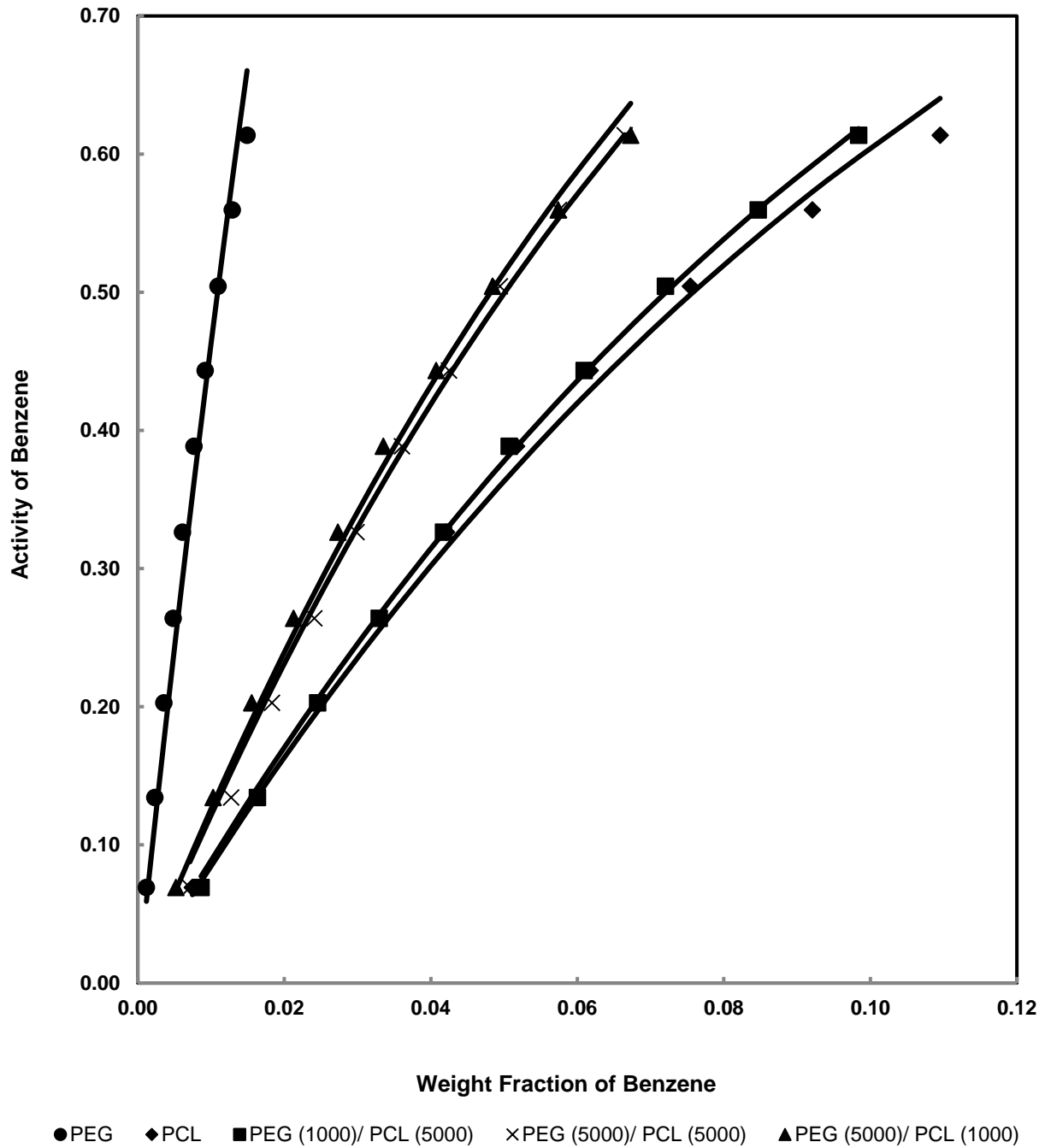
Figure 4.2 Comparison of activity versus weight fraction for benzene in PCL, PEG (1000)/ PCL (5000), PEG (5000)/ PCL (5000), PEG (5000)/ PCL (1000), and PEG at 298.15 K. Solid curves refer to fits to Equation 13
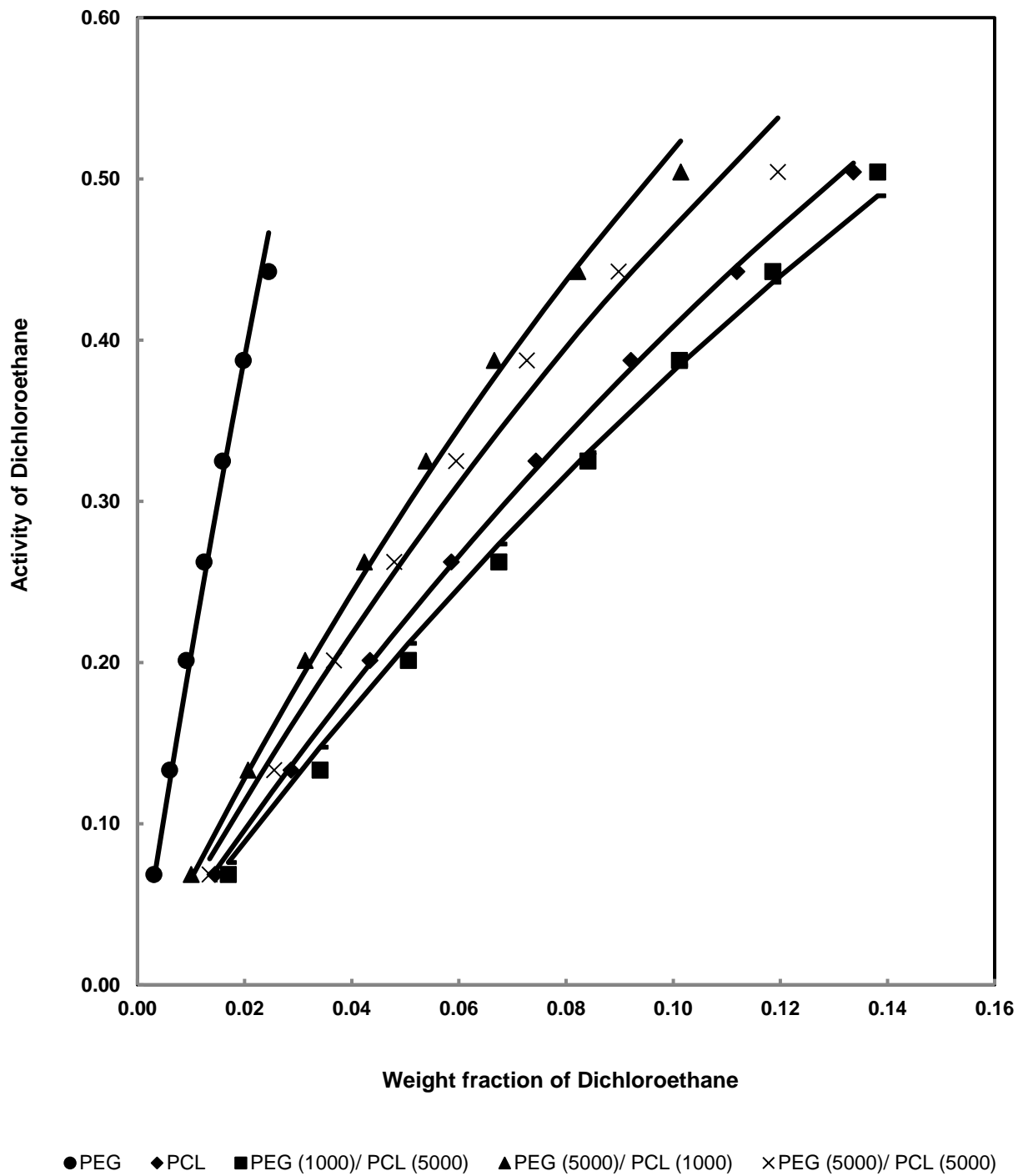
Figure 4.3 Comparison of activity versus weight fraction for DCE in PCL, PEG (1000)/ PCL (5000), PEG (5000)/ PCL (5000), PEG (5000)/ PCL (1000), and PEG at 298.15 K. Solid curves refer to fits to Equation 13
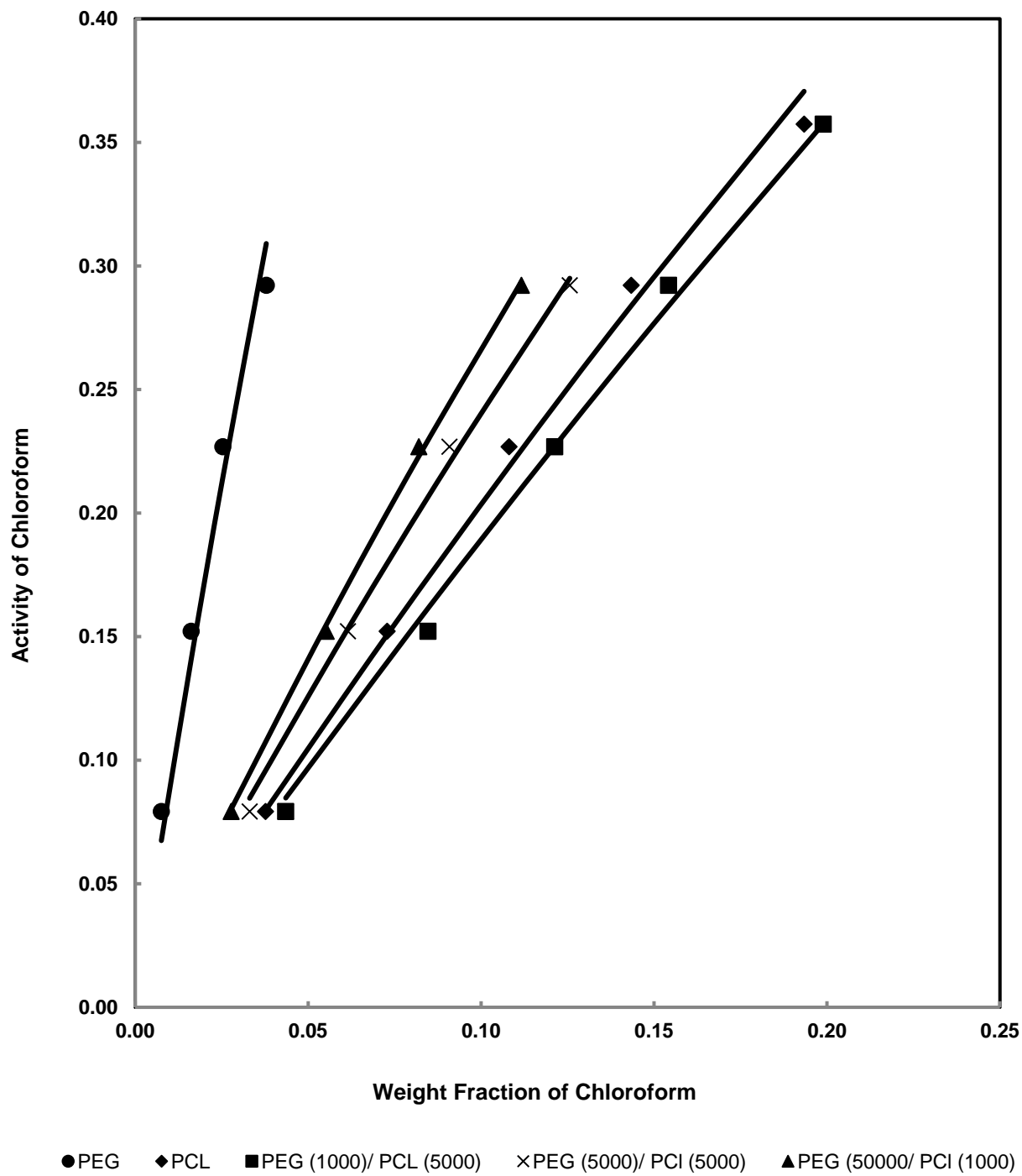
Figure 4.4 Comparison of activity versus weight fraction for chloroform in PCL, PEG (1000)/ PCL (5000), PEG (5000)/ PCL (5000), PEG (5000)/ PCL (1000), and PEG at 298.15 K. Solid curves refer to fits to Equation 13
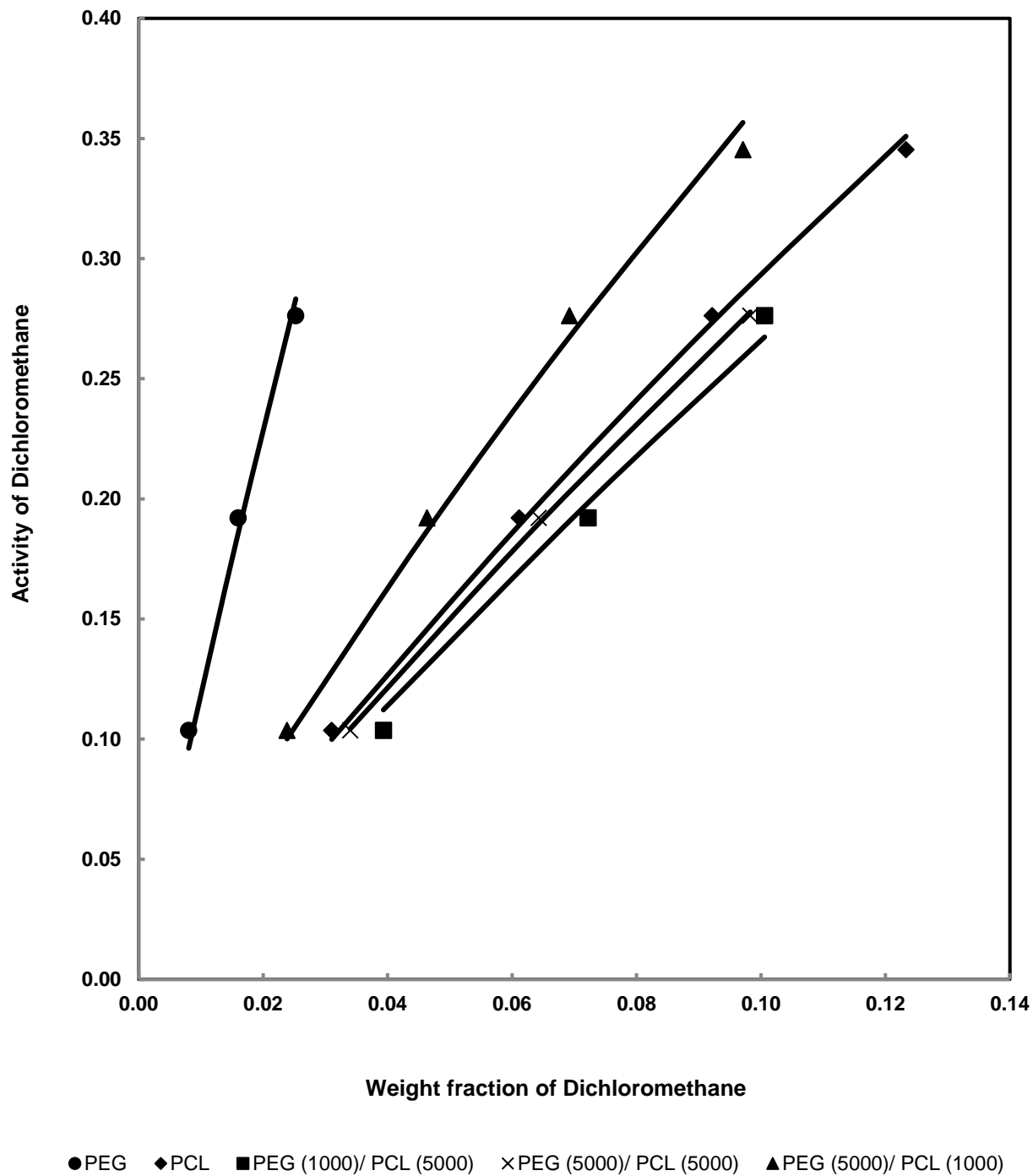
Figure 4.5 Comparison of activity versus weight fraction for DCM in PCL, PEG (1000)/ PCL (5000), PEG (5000)/ PCL (5000), PEG (5000)/ PCL (1000), and PEG at 298.15 K. Solid curves refer to fits to Equation 13

Table 4.6 Parameters used in the Flory-Huggins model

System	X	Δw_1
Benzene-PEG	2.631	0.001
Benzene-PEG (5000)/PCL (1000)	1.263	0.001
Benzene-PEG (5000)/PCL (5000)	1.233	0.001
Benzene-PEG (1000)/PCL (5000)	0.933	0.001
Benzene-PCL	0.884	0.002
DCE-PEG	2.159	0.001
DCE-PEG (5000)/PCL (1000)	0.979	0.002
DCE-PEG (5000)/PCL (5000)	0.868	0.003
DCE-PEG (1000)/PCL (5000)	0.629	0.003
DCE-PCL	0.711	0.001
Chloroform-PEG	1.474	0.002
Chloroform-PEG (5000)/PCL (1000)	0.331	0.001
Chloroform-PEG (5000)/PCL (5000)	0.217	0.002
Chloroform-PEG (1000)/PCL (5000)	-0.044	0.003
Chloroform-PCL	0.039	0.004
DCM-PEG	1.651	0.001
DCM-PEG (5000)/PCL (1000)	0.6	0.002
DCM-PEG (5000)/PCL (5000)	0.295	0
DCM-PEG (1000)/PCL (5000)	0.245	0.003
DCM-PCL	0.363	0.001
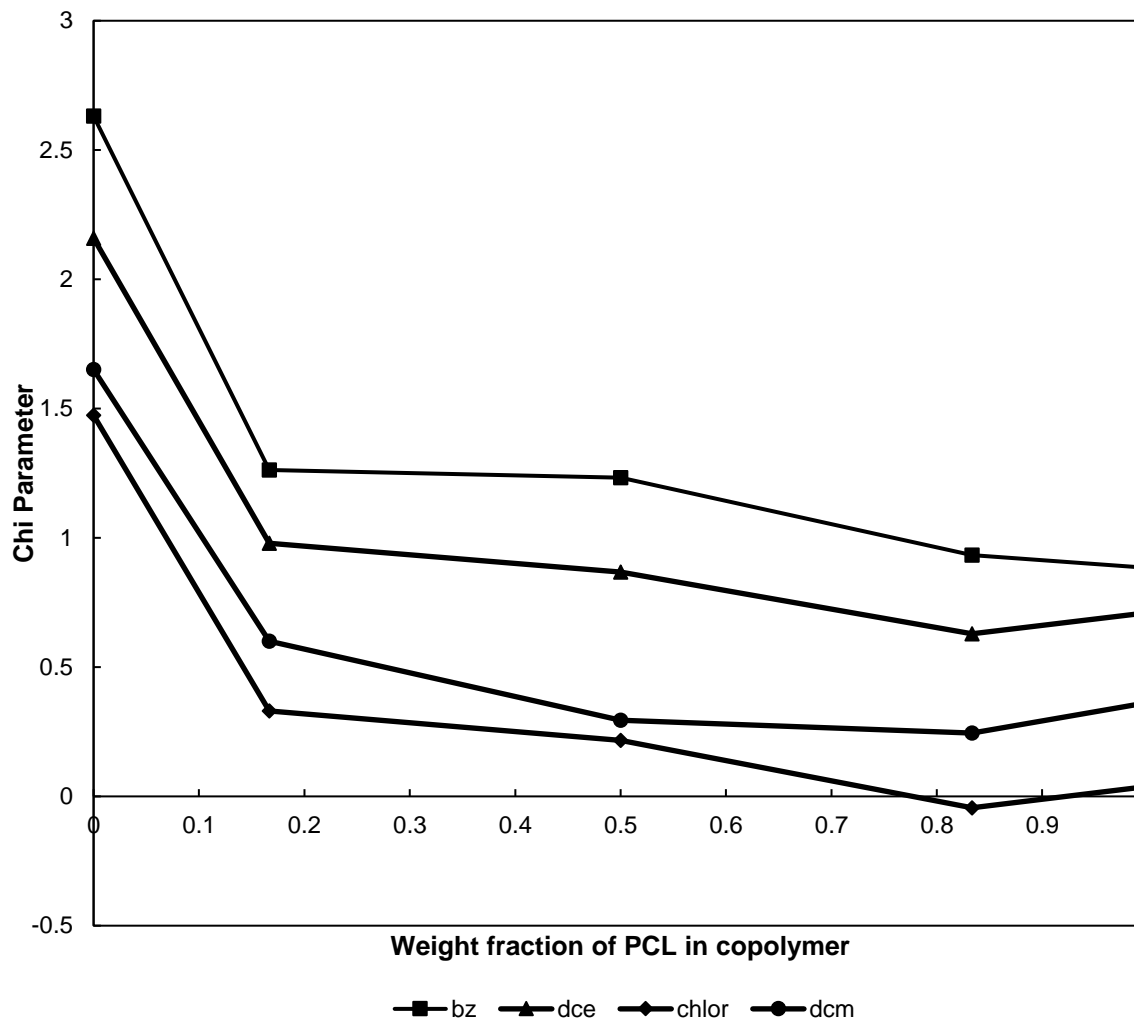
Figure 4.6 Chi parameter vs. weight fraction of PCL in the copolymer

An interesting trend was observed when a plot of chi parameter (polymer solvent interaction parameter used in Flory-Huggins model) versus weight fraction of either of the homopolymer in the copolymer is plotted. The plot between chi parameter for the four solvents and weight fraction of PCL in the copolymer system PCL (1000)/ PEG (5000), PCL (5000)/ PEG (5000), PCL (5000)/ PEG (1000), PCL and PEG show that as the weight fractions of PCL increased, there is a decrease in the chi parameter values for most of the solvents. The figure 4-6 shows the trend.
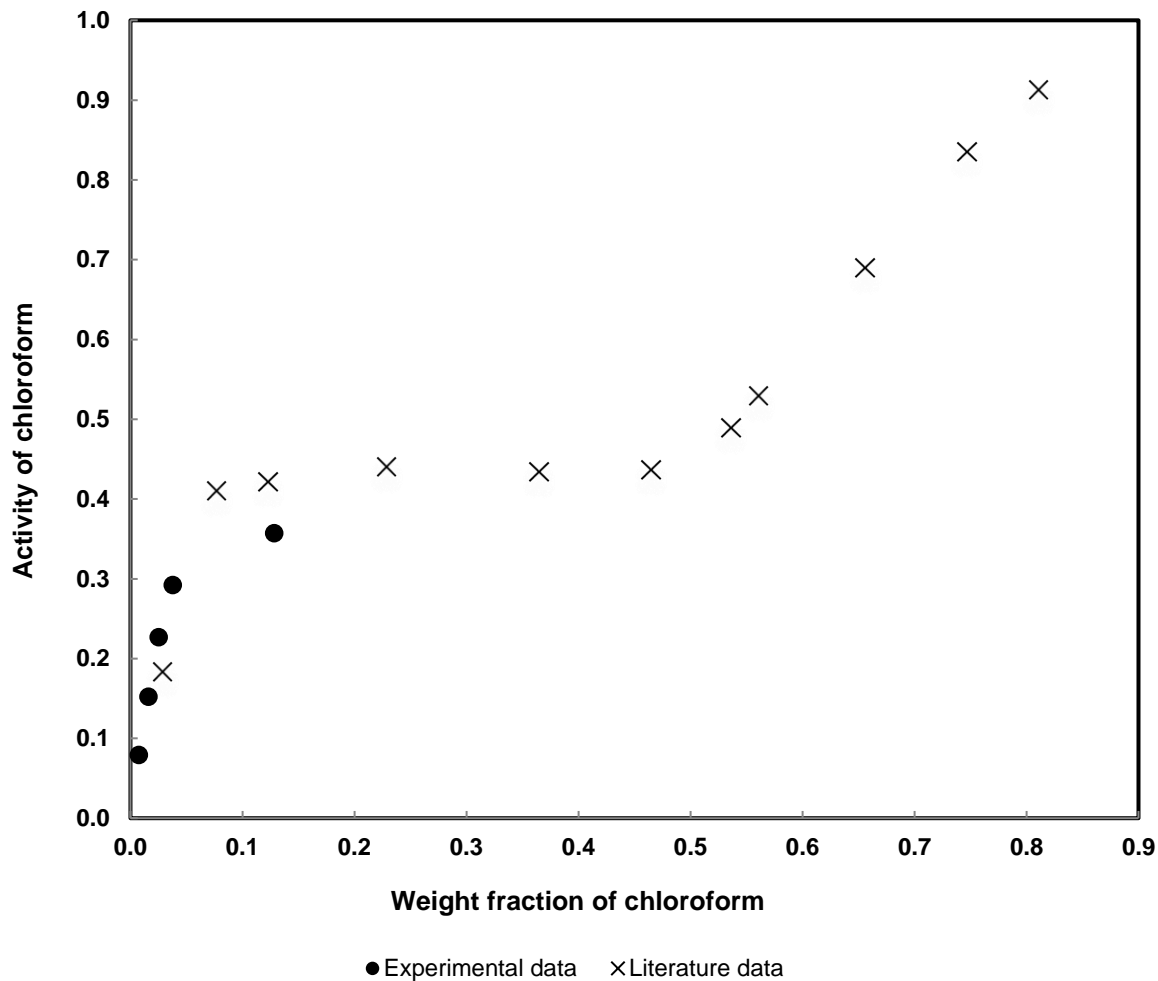
Figure 4.7 Comparison of literature data and experimental data for activity versus weight fraction

plot for chloroform in PEG at 298.15 K

4.2 Discussion

It was noted earlier that, for several runs, the formation of a second polymer-containing

phase occurred at higher solvent weight fractions than reported here. Figure 4-7. shows phase

behavior of chloroform + PEG as determined by Booth et al.[13] at 298 K. Our data for this

system, including an additional data point not reported in Table 4-4, are shown for comparison.

It is clear from Figure 4-7 that a second polymer-containing phase begins to form for chloroform

weight fractions exceeding 0.038. The current technique, as can be seen in Figure 4-7, can

determine that a second phase is formed. However, the resulting activity-weight fraction

measurements are not quantitatively correct, for the second phase appears to be a viscous liquid

and the technique assumes that the polymer film is a solid extension of the quartz crystal.

Resistance measurements support this claim as large resistances indicate viscoelastic effects[23] in

the polymer film. For the runs shown here, the resistance was approximately 10 ohms for the

single-phase measurements but over 200 ohms after the second phase began to form. The

conclusion is that the present technique is accurate if the polymer is inertially coupled to the

piezoelectric surface and does not exhibit viscoelasticity to a significant extent. Thus, we have

reported measurements only for the cases where the resistance is very small, on the order of 10

ohms. Many of the systems included here are expected to exhibit phase splitting as the Flory-

Huggins model leads to phase instability when[24]

$$\chi \geq \frac{1}{2}\left(1+\frac{1}{\sqrt{r}}\right)^2 \quad (20)$$

where $r = V_2/V_1$ is the ratio of molar volumes. This condition is met by about half of the systems

examined here. This can be considered as the limitation of the experimental apparatus to collect

the respective maximum data points for each of the solvents.

CHAPTER 5: CONCLUSION AND FUTURE WORK

5.1 Conclusion

Based on the results of the comparison of literature data and experimental data for PIB polymer, we can conclude that the present equipment setup has the capability to study various polymer-solvent interactions. Solubilities of benzene, dichloroethane, chloroform, and dichloromethane in polyethylene glycol (PEG), polycaprolactone (PCL), and their copolymers (PEG/PCL) at 298.15 K are reported in the form of activity versus weight fraction data and are represented by the Flory-Huggins equation to within experimental accuracy. The QCM technique is shown to identify when phase splitting occurs, and only data for which a single polymer-containing phase exist are reported as the technique is inapplicable when viscoelastic effects are present, as when phase splitting occurs.

5.2 Future Work

Future work consists of repeating the same experiment for triblock copolymers like PCL (5000)/ PEG (5000)/ PCL (5000) and PCL (10,000)/ PEG (5000)/ PCL (10,000) and observing whether they behave similarly to diblock copolymers or not. The other possibility of future work would be to use the present QCM setup to measure diffusion coefficients or to study systems of two solvents and one polymer.

REFERENCES

1. King, W. H., Piezoelectric Sorption Detector. *Analytical Chemistry* 1964, 36, (9), 1735-1739.

2. Masouka, H., N. Murashige, and M. Yorizane, Fluid Phase Equilibria., 1B, 155 (1984).

3. Woodruff, M. A.; Hutmacher, D. W., The return of a forgotten polymer—Polycaprolactone in the 21st century. *Progress in Polymer Science* 2010, 35, (10), 1217-1256.

4. Shen-Guo, Wang, and Qiu Bo. "Polycaprolactone-Poly (ethylene Glycol) Block Copolymer, I: Synthesis and Degradability in Vitro." Polymers for Advanced Technologies 4.6 (1993): 363-66.

5. Wong, H. C.; Campbell, S. W.; Bhethanabotla, V. R., Sorption of Benzene, Dichloromethane, and 2-Butanone by Poly (methyl methacrylate), Poly (butyl methacrylate), and Their Copolymers at 323.15 K Using a Quartz Crystal Balance. *Journal of Chemical & Engineering Data* 2016, 61, (11), 3877-3882.

6. Wong, H. C.; Campbell, S. W.; Bhethanabotla, V. R., Sorption of benzene, toluene and chloroform by poly(styrene) at 298.15 K and 323.15 K using a quartz crystal balance. *Fluid Phase Equilibria* 1997, 139, (1–2), 371-389.

7. Wong, H. C.; Campbell, S. W.; Bhethanabotla, V. R., Sorption of benzene, tetrahydrofuran and 2-butanone by poly (vinyl acetate) at 323.15 K using a quartz crystal balance. *Fluid Phase Equilibria* 2001, 179, (1–2), 181-191.

8. Wong, H. C.; Campbell, S. W.; Bhethanabotla, V. R., Sorption of Benzene, Dichloromethane, n-Propyl Acetate, and 2-Butanone by Poly (methyl methacrylate), Poly (ethyl methacrylate), and Their Copolymers at 323.15 K Using a Quartz Crystal Balance. *Journal of Chemical & Engineering Data* 2011, 56, (12), 4772-4777.

9. Koleske, J. V., and R. D. Lundberg. "Lactone Polymers. I. Glass Transition Temperature of Poly-É›-caprolactone by Means on Compatible Polymer Mixtures." Journal of Polymer Science Part A-2: Polymer Physics 7.5 (1969): 795-807.

10. Pitt, C. G.; Jeffcoat, A. R.; Zweidinger, R. A.; Schindler, A., Sustained drug delivery systems. I. The permeability of poly(epsilon-caprolactone), poly (DL-lactic acid), and their copolymers. *J Biomed Mater Res* 1979, 13, (3), 497-507.

11. Inada, Yuji, Katsunobu Takahashi, Takayuki Yoshimoto, Ayako Ajima, Ayako Matsushima, and Yuji Saito. "Application of Polyethylene Glycol-modified Enzymes in Biotechnological Processes: Organic Solvent-soluble Enzymes." Trends in Biotechnology 4.7 (1986): 190-94.

12. Sauerbrey, G., Use of oscillating quartz for weighing thin layers and for microwaving. *Magazine for Physics* April 1959, 155, (2), 206-222.

13. Mikkilineni, Siva Prasad, Alan Tree, and Martin High. Thermophysical Properties of Penetrants in Polymers via a Piezoelectric Quartz Crystal Microbalance. N.p.: J. Chem. Eng. Data, 1995.

14. Rodahl, Michael, Fredrik Hook, Anatol Krozer, Peter Brzezinski, and Bengt Kasemo. "Quartz Crystal Microbalance Setup for Frequency and Q-factor Measurements in Gaseous and Liquid Environments." Review of Scientific Instruments 66.7 (1995): 3924-930.

15. Panayiotou, C.; Vera, J. H., Thermodynamics of Polymer-Polymer-Solvent and Block Copolymer-Solvent Systems I. Experimental Measurements. *Polym J* 1984, 16, (2), 89-102.

16. Wen Hao, H. S. E., P. Alessi, *Polymer Solution Data Collection*. 1992; Vol. XIV.

17. Booth, C.; Gee, G.; Holden, G.; Williamson, G. R., Studies in the thermodynamics of polymer-liquid systems. *Polymer* 1964, 5, 343-370.

18. Tsonopoulos, C., An empirical correlation of second virial coefficients. *AIChE Journal* 1974, 20, (2), 263-272.

19. Meng, L.; Duan, Y.-Y., Prediction of the second cross virial coefficients of nonpolar binary mixtures. *Fluid Phase Equilibria* 2005, 238, (2), 229-238.

20. Dymond, J. H.; Smith, E. B., *The virial coefficients of pure gases and mixtures: a crit. compilation*. Clarendon Pr.: Oxford, 1980.

21. (NIST), N. I. o. S. a. T. Antoine Equation Parameters. http://webbook.nist.gov/chemistry/ (08/24/2016).

22. Stephen Martin, Victoria Edwards Granstaff and Gregory C. Frye, "Characterization of a Quartz Crystal Microbalance with Simultaneous Mass and Liquid Loading", Anal. Chem. 63 (1991) 2272.

23. Diethelm Johannsmann, "Viscoelastic Analysis of Organic Thin Films" on quartz resonators", Macromol. Chem. Phys. 200(1999)501.

24. Prausnitz, J. M. L., Rudiger N.; de Azevedo, Edmundo Gomes, *Molecular Thermodynamics of Fluid-Phase Equilibria- Third edition*. Third ed.; Prentice Hall: New Jersey, 1998.

APPENDIX A: ADDITIONAL INFORMATION

The detailed information regarding the sorption process by LabView software is listed below in this section. Each of the bubblers has one solvent each and they are represented as Bubbler 1- Benzene, Bubbler 2- DCE, Bubbler 3- Chloroform, Bubbler 4- DCM. The standard deviation in frequency, resistance and weight fraction are also calculated by the LabView software. The LabView software automates the overall experiment by controlling the flow of nitrogen to the bubblers and collecting the valid data points in the form of resistance, frequency, weight fraction and the deviations in each of them. The acceptable resistance range was from 10-20 ohms for the runs done here.

Table A.1 Metadata file for sorption of benzene in PEG at 298.15 K

Time	Bubbler	Event	Resistance mean	Resistance standard deviation	Frequency mean	Frequency standard deviation	Weight fraction	Weight fraction standard deviation
203.3483	1	Purge	11.801	0.026	4994195.580	0.499		
394.4904	1	1	11.874	0.024	4994193.120	0.558	0.001	0.000
561.1811	1	2	11.919	0.028	4994190.680	0.471	0.002	0.000
735.7326	1	3	11.955	0.027	4994188.140	0.535	0.004	0.000
891.9772	1	4	12.004	0.029	4994185.460	0.579	0.005	0.000
1023.909	1	5	12.056	0.029	4994182.800	0.452	0.006	0.000
1178.593	1	6	12.114	0.026	4994179.480	0.505	0.008	0.000
1333.19	1	7	12.192	0.030	4994176.180	0.482	0.009	0.000
1524.278	1	8	12.272	0.026	4994172.460	0.542	0.011	0.000
1695.67	1	9	12.379	0.027	4994168.300	0.544	0.013	0.000
1812.417	1	10	12.473	0.030	4994163.940	0.424	0.015	0.000

Table A.2 Metadata file for sorption of DCE, chloroform and DCM in PEG at 298.15 K

Time	Bubbler	Event	Resistance mean	Resistance standard deviation	Frequency mean	Frequency standard deviation	Weight fraction	Weight fraction standard deviation
138.577	0.000	Baseline	10.289	0.026	4998349.160	0.510	-	-
1392.450	1.000	Purge	16.679	0.032	4997661.640	0.485	-	-
1530.592	1.000	1.000	17.018	0.029	4997656.480	0.505	0.007	0.001
1662.583	1.000	2.000	17.246	0.035	4997650.240	0.476	0.016	0.001
1771.766	1.000	3.000	17.497	0.032	4997644.280	0.454	0.025	0.001
1944.769	1.000	4.000	17.712	0.035	4997637.920	0.528	0.033	0.001
2064.750	1.000	5.000	17.939	0.030	4997631.400	0.495	0.042	0.001
2306.003	1.000	6.000	18.168	0.035	4997624.140	0.452	0.052	0.001
2406.225	1.000	7.000	18.174	0.035	4997616.400	0.535	0.062	0.001
2506.297	1.000	8.000	18.009	0.031	4997605.560	0.541	0.075	0.001
2682.332	1.000	9.000	18.296	0.041	4997591.900	0.416	0.092	0.001
2814.464	1.000	10.000	19.558	0.039	4997577.080	0.488	0.110	0.001
2998.004	2.000	Purge	16.818	0.031	4997661.680	0.551		
3236.208	2.000	1.000	17.206	0.035	4997651.580	0.499	0.014	0.001
3325.646	2.000	2.000	17.622	0.035	4997641.420	0.538	0.029	0.001
3413.606	2.000	3.000	17.910	0.028	4997630.500	0.505	0.043	0.001
3594.100	2.000	4.000	18.099	0.034	4997618.900	0.463	0.059	0.001
3704.892	2.000	5.000	18.012	0.033	4997606.460	0.503	0.074	0.001
3867.222	2.000	6.000	17.917	0.037	4997591.940	0.424	0.092	0.001
4037.187	2.000	7.000	18.136	0.036	4997575.080	0.488	0.112	0.001
4307.623	2.000	8.000	18.994	0.036	4997555.620	0.530	0.134	0.001
4512.461	3.000	Purge	16.768	0.031	4997661.260	0.600		
4797.607	3.000	1.000	17.641	0.028	4997634.320	0.551	0.038	0.001
4931.193	3.000	2.000	18.087	0.034	4997607.200	0.571	0.073	0.001
5266.953	3.000	3.000	17.960	0.032	4997577.920	0.528	0.108	0.001
5412.782	3.000	4.000	18.666	0.040	4997546.080	0.444	0.143	0.001
6090.093	3.000	5.000	23.649	0.041	4997496.340	0.519	0.193	0.001
6272.200	4.000	Purge	17.084	0.036	4997660.740	0.600		
6471.065	4.000	1.000	17.944	0.034	4997638.700	0.544	0.031	0.001
6622.900	4.000	2.000	17.963	0.035	4997615.920	0.601	0.061	0.001
6950.774	4.000	3.000	18.209	0.035	4997590.860	0.405	0.092	0.001
7196.638	4.000	4.000	19.943	0.035	4997563.920	0.488	0.123	0.001

Table A.3 Metadata file for sorption of benzene, DCE, chloroform, and DCM in PCL at 298.15

K

Time	Bubbler	Event	Resistance mean	Resistance standard deviation	Frequency mean	Frequency standard deviation	Weight fraction	Weight fraction standard deviation
185.285	1.000	Purge	12.302	0.030	4999315.300	0.544	-	-
400.901	1.000	1.000	12.186	0.029	4999295.780	0.507	0.005	0.000
499.615	1.000	2.000	12.146	0.031	4999276.500	0.505	0.010	0.000
601.341	1.000	3.000	12.145	0.029	4999256.340	0.557	0.016	0.000
757.563	1.000	4.000	12.136	0.027	4999234.180	0.596	0.021	0.000
1004.741	1.000	5.000	12.112	0.027	4999210.380	0.567	0.027	0.000
1114.113	1.000	6.000	12.107	0.026	4999185.780	0.465	0.034	0.000
1399.501	1.000	7.000	12.096	0.029	4999156.800	0.606	0.041	0.000
1577.040	1.000	8.000	12.125	0.029	4999125.360	0.525	0.048	0.000
1891.394	1.000	9.000	12.174	0.028	4999087.920	0.444	0.057	0.000
2207.105	1.000	10.000	12.335	0.030	4999045.900	0.505	0.067	0.000
2422.538	2.000	Purge	11.822	0.026	4999314.320	0.471		
2893.357	2.000	1.000	11.891	0.029	4999276.440	0.787	0.010	0.000
3029.965	2.000	2.000	11.891	0.029	4999235.680	0.794	0.021	0.000
3177.230	2.000	3.000	11.949	0.031	4999193.700	0.763	0.031	0.000
3403.480	2.000	4.000	12.030	0.029	4999149.060	0.586	0.042	0.000
3542.976	2.000	5.000	12.110	0.028	4999101.780	0.679	0.054	0.000
3741.800	2.000	6.000	12.231	0.031	4999047.900	0.544	0.067	0.000
4120.178	2.000	7.000	12.559	0.029	4998979.900	0.505	0.082	0.000
4331.394	2.000	8.000	13.091	0.030	4998892.880	0.594	0.101	0.000
4530.140	3.000	Purge	11.752	0.032	4999313.440	0.611		
5477.755	3.000	1.000	11.743	0.031	4999206.760	1.021	0.028	0.000
5595.233	3.000	2.000	11.882	0.031	4999095.140	0.670	0.055	0.000
5865.813	3.000	3.000	12.159	0.030	4998979.880	0.773	0.082	0.000
6564.341	3.000	4.000	12.752	0.031	4998843.900	0.707	0.112	0.000
7511.943	3.000	5.000	15.881	0.031	4998508.600	3.194	0.177	0.001
7796.847	4.000	Purge	11.086	0.029	4999311.460	0.542		
8033.452	4.000	1.000	11.492	0.029	4999220.160	0.792	0.024	0.000
8229.082	4.000	2.000	11.836	0.028	4999129.820	0.560	0.046	0.000
8526.228	4.000	3.000	12.337	0.029	4999033.440	0.644	0.069	0.000
9265.582	4.000	4.000	13.208	0.031	4998909.500	0.580	0.097	0.000

Table A.4 Metadata file for sorption of benzene, DCE, chloroform and DCM in PEG (5000)/

PCL (1000) at 298.15 K

Time	Bubbler	Event	Resistance mean	Resistance standard deviation	Frequency mean	Frequency standard deviation	Weight fraction	Weight fraction standard deviation
103.844	1.000	Purge	16.473	0.031	5000937.880	0.521		
319.989	1.000	1.000	16.518	0.031	5000926.580	0.499	0.009	0.001
472.412	1.000	2.000	16.459	0.029	5000916.340	0.593	0.016	0.001
558.239	1.000	3.000	16.412	0.034	5000905.240	0.476	0.025	0.001
670.863	1.000	4.000	16.349	0.036	5000893.720	0.497	0.033	0.001
770.090	1.000	5.000	16.293	0.030	5000881.400	0.571	0.042	0.001
857.566	1.000	6.000	16.229	0.034	5000868.640	0.663	0.051	0.001
1002.688	1.000	7.000	16.186	0.032	5000853.760	0.476	0.061	0.000
1298.917	1.000	8.000	16.111	0.031	5000837.240	0.625	0.072	0.001
1455.965	1.000	9.000	16.100	0.034	5000817.900	0.463	0.085	0.000
1592.313	1.000	10.000	16.116	0.036	5000796.380	0.567	0.098	0.001
1761.116	2.000	Purge	16.311	0.035	5000936.300	0.544		
2098.692	2.000	1.000	16.383	0.032	5000913.900	0.735	0.017	0.001
2205.325	2.000	2.000	16.367	0.037	5000890.520	0.707	0.034	0.001
2306.047	2.000	3.000	16.338	0.032	5000867.160	0.584	0.051	0.001
2449.687	2.000	4.000	16.286	0.033	5000842.400	0.571	0.067	0.001
2602.172	2.000	5.000	16.255	0.037	5000817.100	0.544	0.084	0.001
2722.165	2.000	6.000	16.233	0.032	5000790.220	0.582	0.101	0.001
2848.006	2.000	7.000	16.211	0.035	5000761.660	0.593	0.119	0.001
3044.951	2.000	8.000	16.216	0.033	5000728.160	0.548	0.138	0.000
3305.578	3.000	Purge	16.367	0.034	5000936.280	0.454		
3618.178	3.000	1.000	16.366	0.031	5000877.200	0.606	0.044	0.001
3763.234	3.000	2.000	16.353	0.034	5000816.180	0.596	0.085	0.001
3927.694	3.000	3.000	16.296	0.035	5000757.060	0.620	0.121	0.000
4133.398	3.000	4.000	16.307	0.031	5000699.560	0.787	0.154	0.001
4426.400	3.000	5.000	16.362	0.034	5000613.940	0.767	0.199	0.000
4645.481	4.000	Purge	16.432	0.037	5000935.620	0.490		
4907.568	4.000	1.000	16.427	0.031	5000882.460	0.542	0.039	0.001
5049.704	4.000	2.000	16.436	0.028	5000834.520	0.707	0.072	0.001
5197.798	4.000	3.000	16.380	0.032	5000790.380	0.567	0.101	0.000
5356.297	4.000	4.000	16.382	0.031	5000745.320	0.513	0.128	0.000

Table A.5 Metadata file for sorption of benzene, DCE, chloroform, and DCM in PEG (1000)/

PCL (5000) at 298.15 K

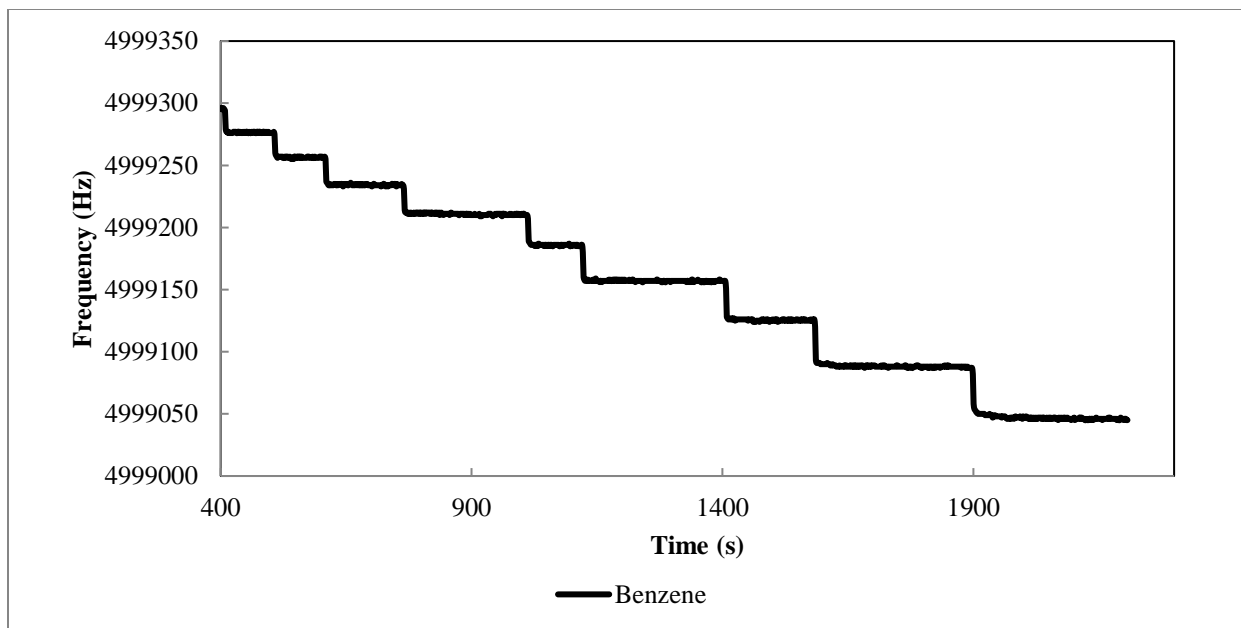| Time	Bubbler	Event	Resistance mean	Resistance standard deviation	Frequency mean	Frequency standard deviation	Weight fraction	Weight fraction standard deviation
103.844	1.000	Purge	16.473	0.031	5000937.880	0.521		
319.989	1.000	1.000	16.518	0.031	5000926.580	0.499	0.009	0.001
472.412	1.000	2.000	16.459	0.029	5000916.340	0.593	0.016	0.001
558.239	1.000	3.000	16.412	0.034	5000905.240	0.476	0.025	0.001
670.863	1.000	4.000	16.349	0.036	5000893.720	0.497	0.033	0.001
770.090	1.000	5.000	16.293	0.030	5000881.400	0.571	0.042	0.001
857.566	1.000	6.000	16.229	0.034	5000868.640	0.663	0.051	0.001
1002.688	1.000	7.000	16.186	0.032	5000853.760	0.476	0.061	0.000
1298.917	1.000	8.000	16.111	0.031	5000837.240	0.625	0.072	0.001
1455.965	1.000	9.000	16.100	0.034	5000817.900	0.463	0.085	0.000
1592.313	1.000	10.000	16.116	0.036	5000796.380	0.567	0.098	0.001
1761.116	2.000	Purge	16.311	0.035	5000936.300	0.544		
2098.692	2.000	1.000	16.383	0.032	5000913.900	0.735	0.017	0.001
2205.325	2.000	2.000	16.367	0.037	5000890.520	0.707	0.034	0.001
2306.047	2.000	3.000	16.338	0.032	5000867.160	0.584	0.051	0.001
2449.687	2.000	4.000	16.286	0.033	5000842.400	0.571	0.067	0.001
2602.172	2.000	5.000	16.255	0.037	5000817.100	0.544	0.084	0.001
2722.165	2.000	6.000	16.233	0.032	5000790.220	0.582	0.101	0.001
2848.006	2.000	7.000	16.211	0.035	5000761.660	0.593	0.119	0.001
3044.951	2.000	8.000	16.216	0.033	5000728.160	0.548	0.138	0.000
3305.578	3.000	Purge	16.367	0.034	5000936.280	0.454		
3618.178	3.000	1.000	16.366	0.031	5000877.200	0.606	0.044	0.001
3763.234	3.000	2.000	16.353	0.034	5000816.180	0.596	0.085	0.001
3927.694	3.000	3.000	16.296	0.035	5000757.060	0.620	0.121	0.000
4133.398	3.000	4.000	16.307	0.031	5000699.560	0.787	0.154	0.001
4426.400	3.000	5.000	16.362	0.034	5000613.940	0.767	0.199	0.000
4645.481	4.000	Purge	16.432	0.037	5000935.620	0.490		
4907.568	4.000	1.000	16.427	0.031	5000882.460	0.542	0.039	0.001
5049.704	4.000	2.000	16.436	0.028	5000834.520	0.707	0.072	0.001
5197.798	4.000	3.000	16.380	0.032	5000790.380	0.567	0.101	0.000
5356.297	4.000	4.000	16.382	0.031	5000745.320	0.513	0.128	0.000

Figure A.1 Frequency-time curve for sorption of benzene in PEG (5000)/ PCL (1000) at 298.15
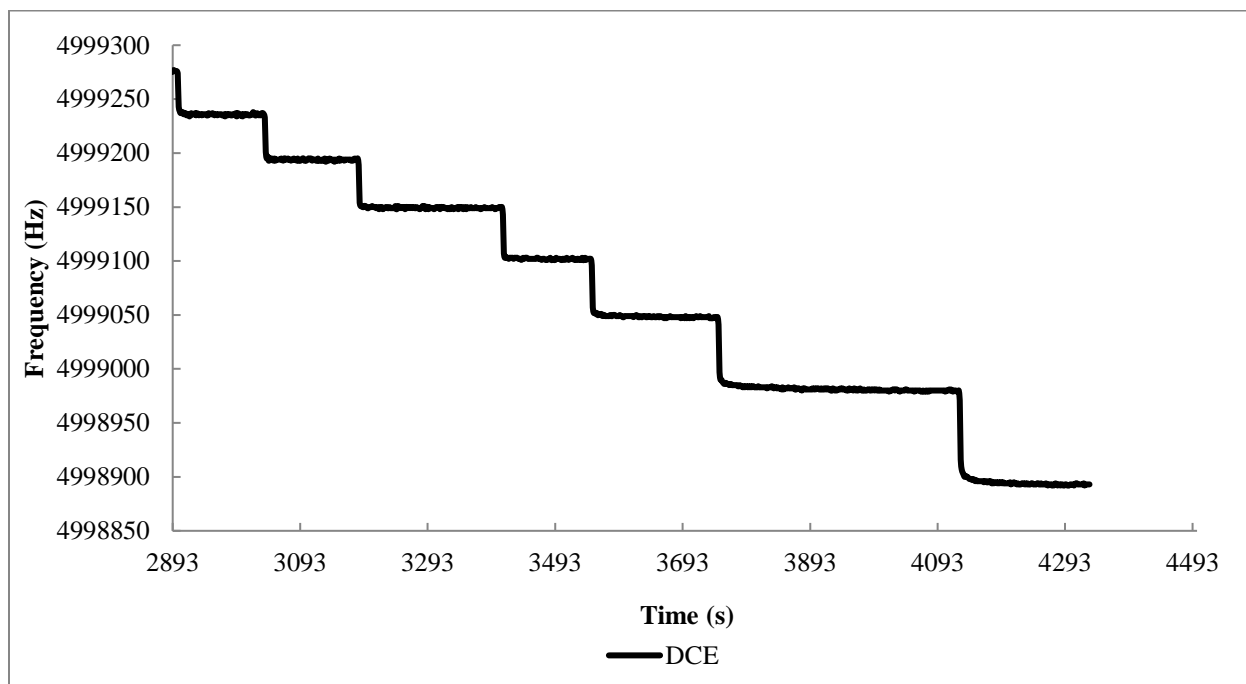
K

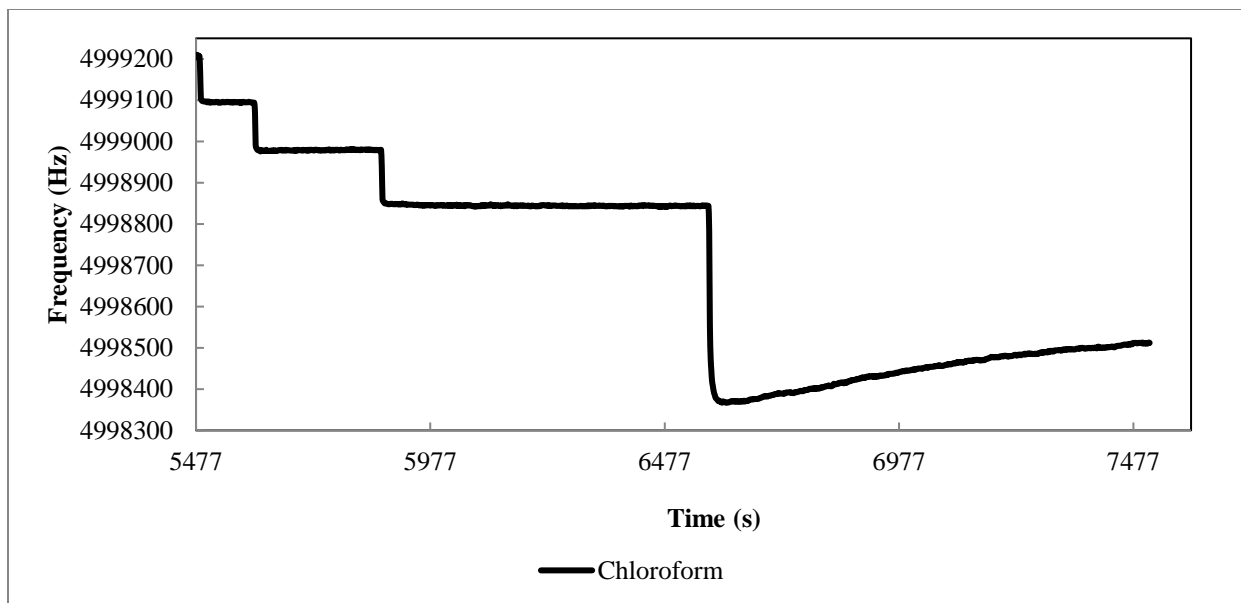Figure A.2 Frequency-time curve for sorption of DCE in PEG (5000)/ PCL (1000) at 298.15 K

47

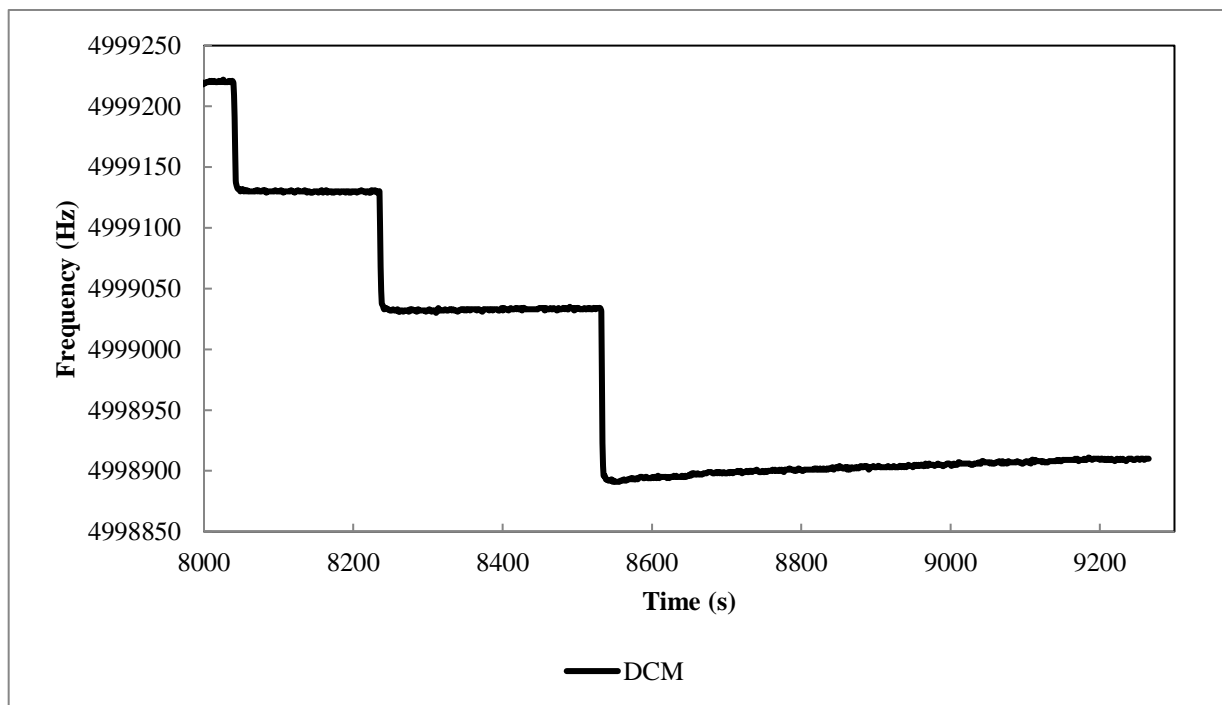Figure A.3 Frequency-time curve for sorption of chloroform in PEG (5000)/ PCL (1000) at

298.15 K

Figure A.4 Frequency-time curve for sorption of DCM in PEG (5000)/ PCL (1000) at 298.15 K
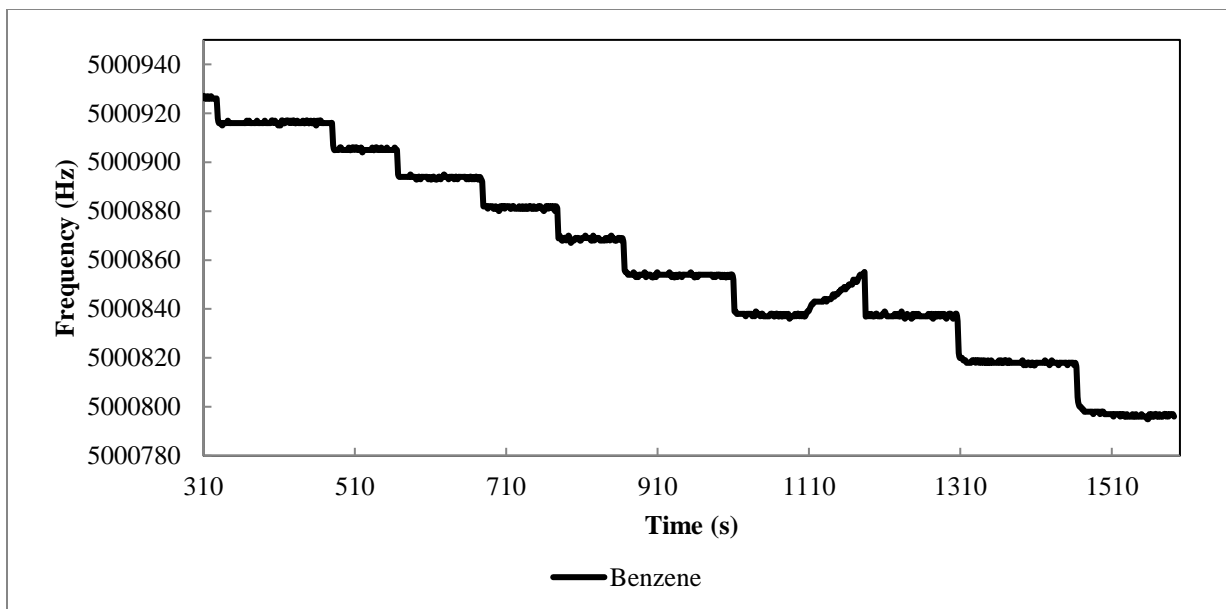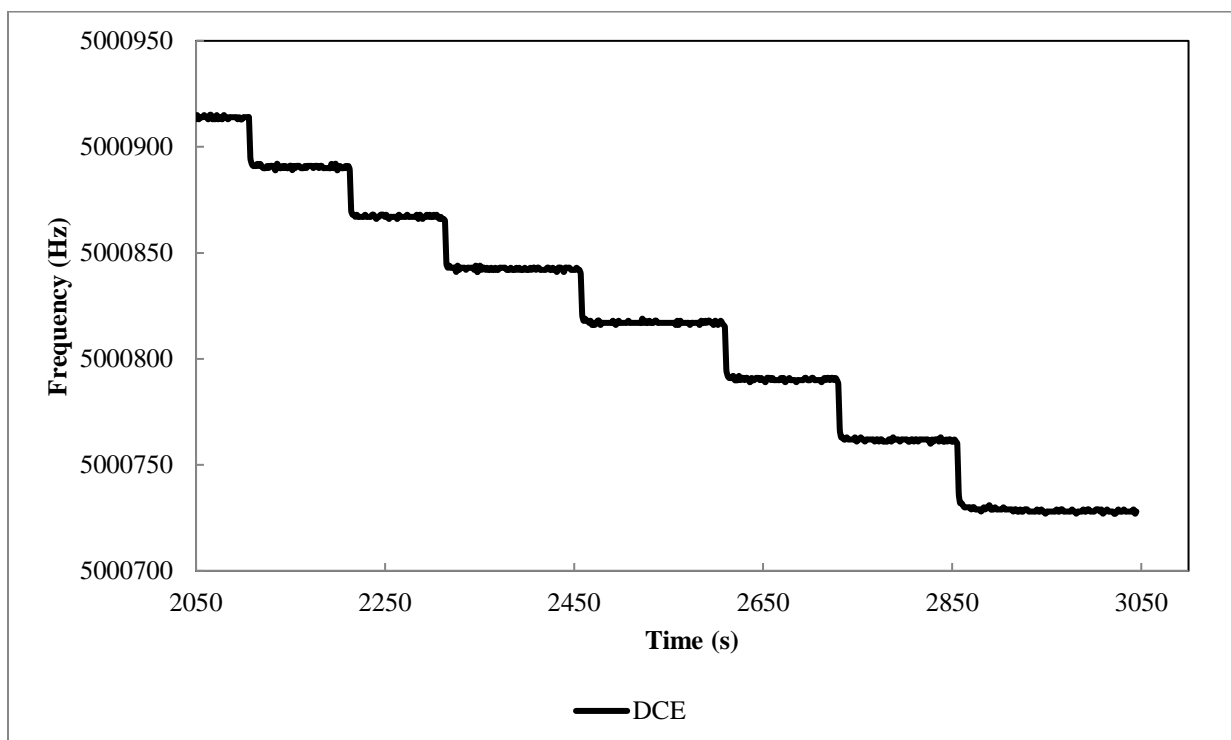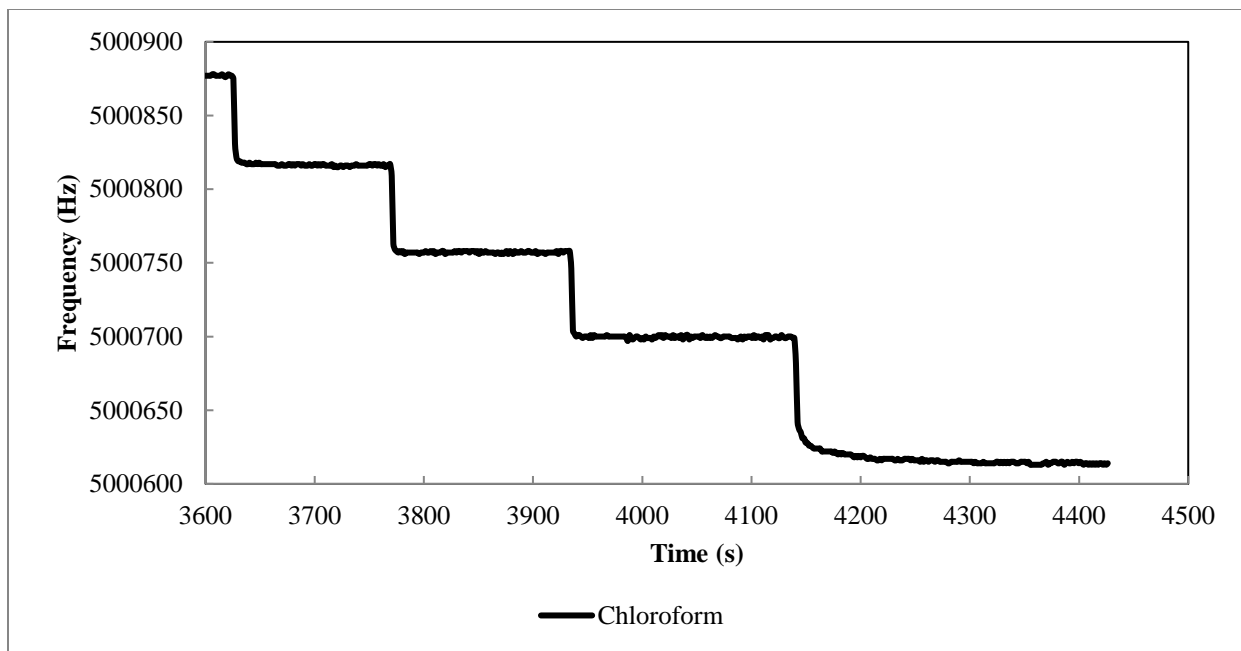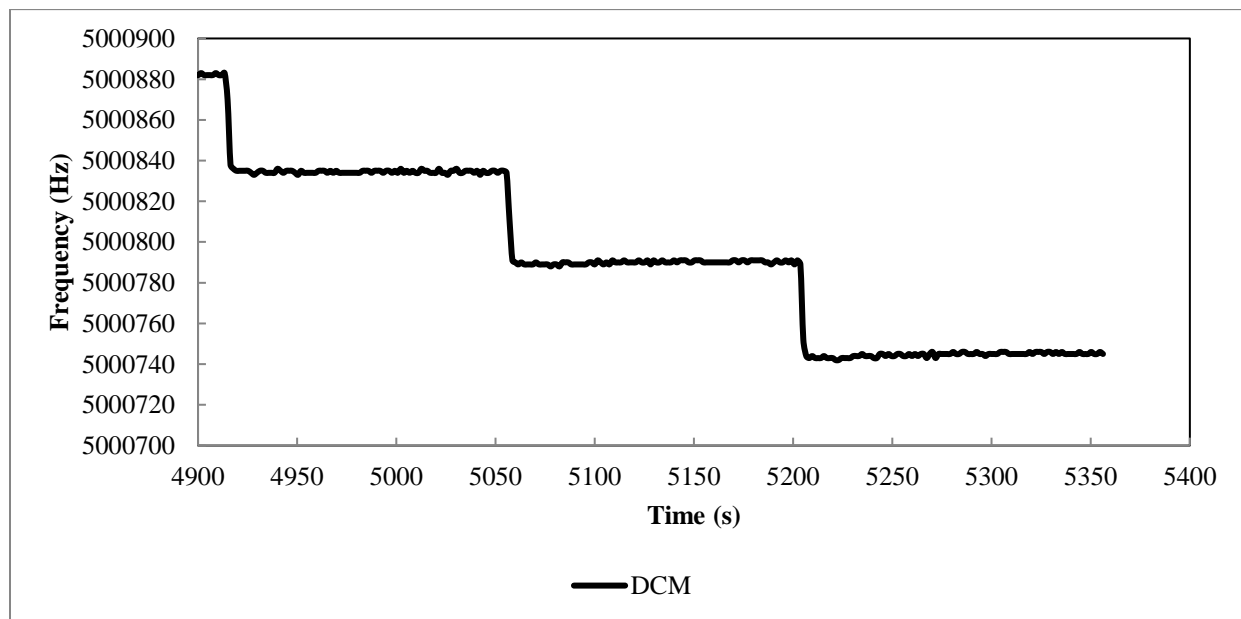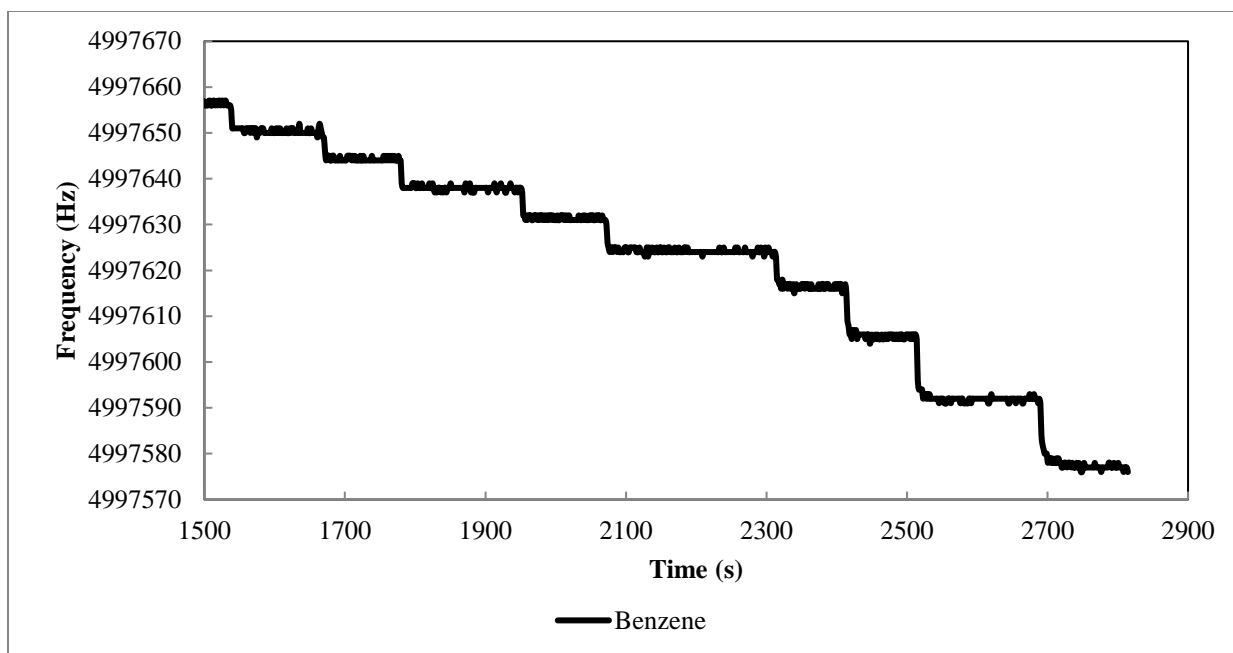
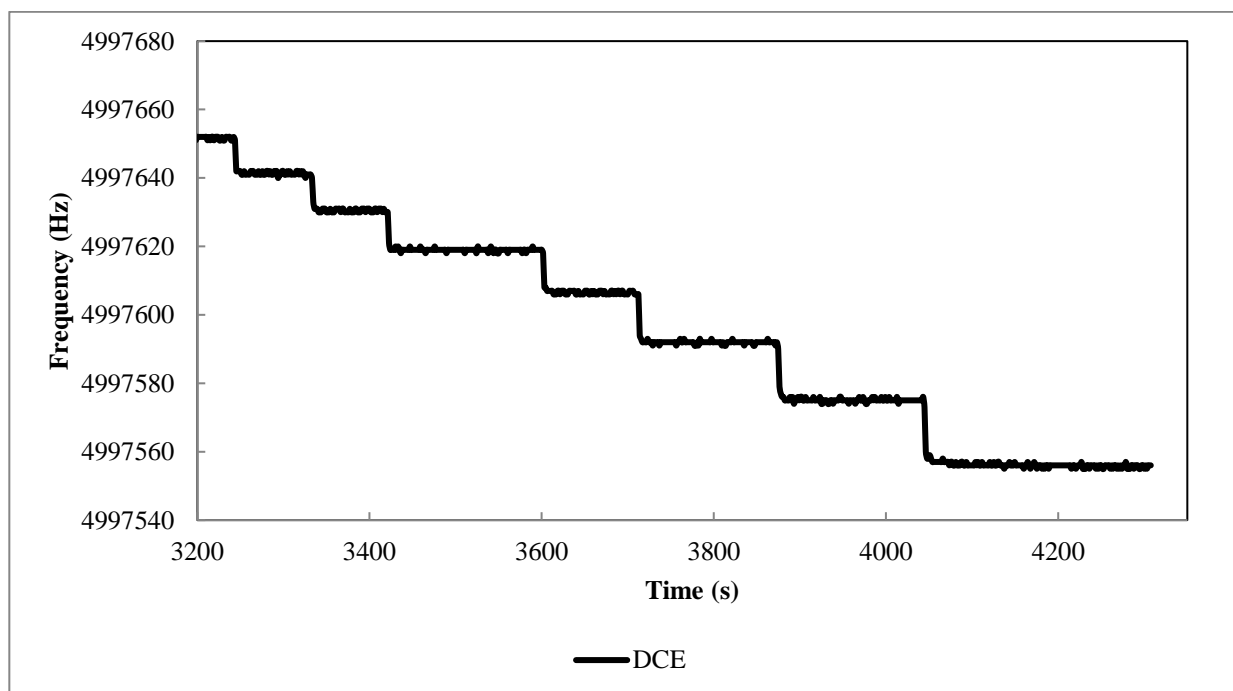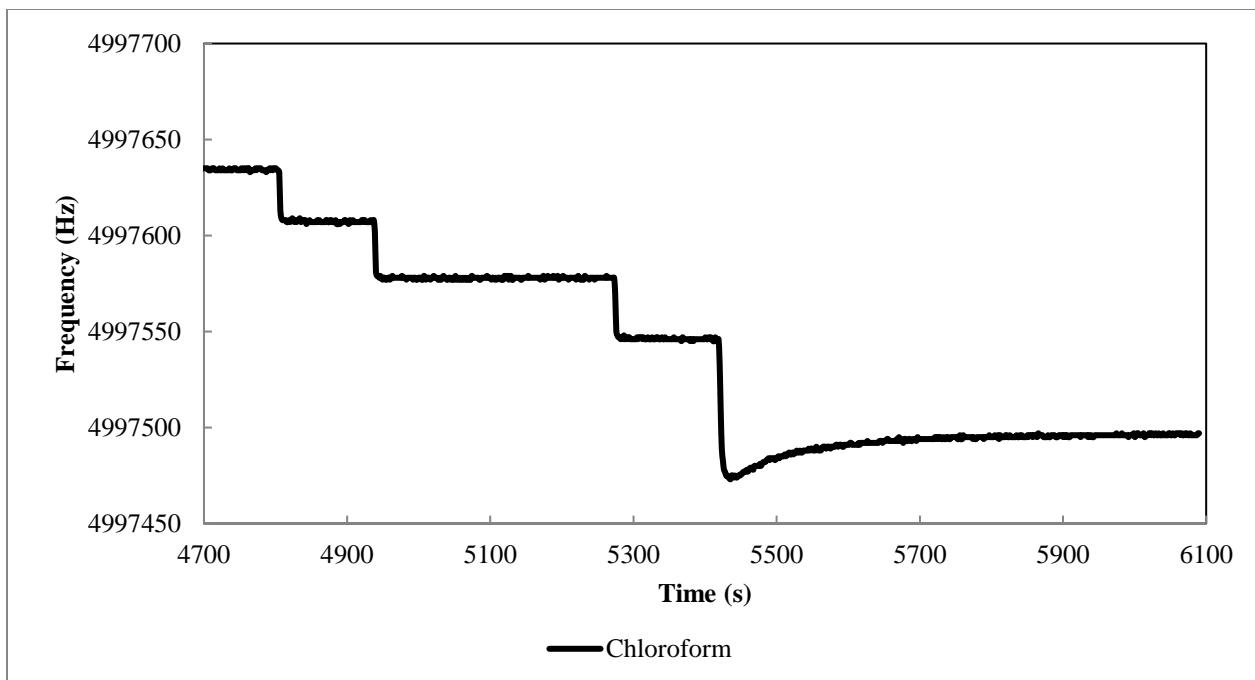Figure A.5 Frequency-time curve for sorption of benzene in PEG (1000)/ PCL (5000) at 298.15

K

Figure A.6 Frequency-time curve for sorption of DCE in PEG (1000)/ PCL (5000) at 298.15 K

Figure A.7 Frequency-time curve for sorption of chloroform in PEG (1000)/ PCL (5000) at

298.15 K

Figure A.8 Frequency-time curve for sorption of DCM in PEG (1000)/ PCL (5000) at 298.15 K

50

Figure A.9 Frequency-time curve for sorption of benzene in PCL at 298.15 K

Figure A.10 Frequency-time curve for sorption of DCE in PCL at 298.15 K

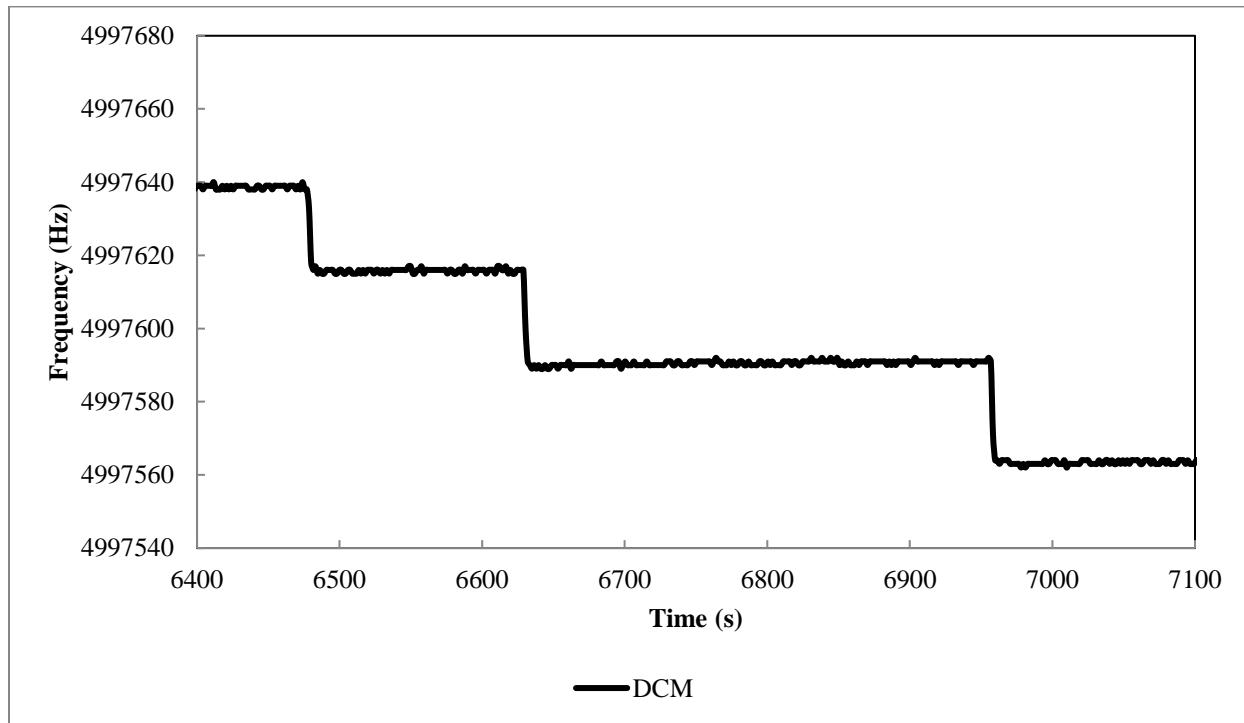Figure A.11 Frequency-time curve for sorption of chloroform in PCL at 298.15 K

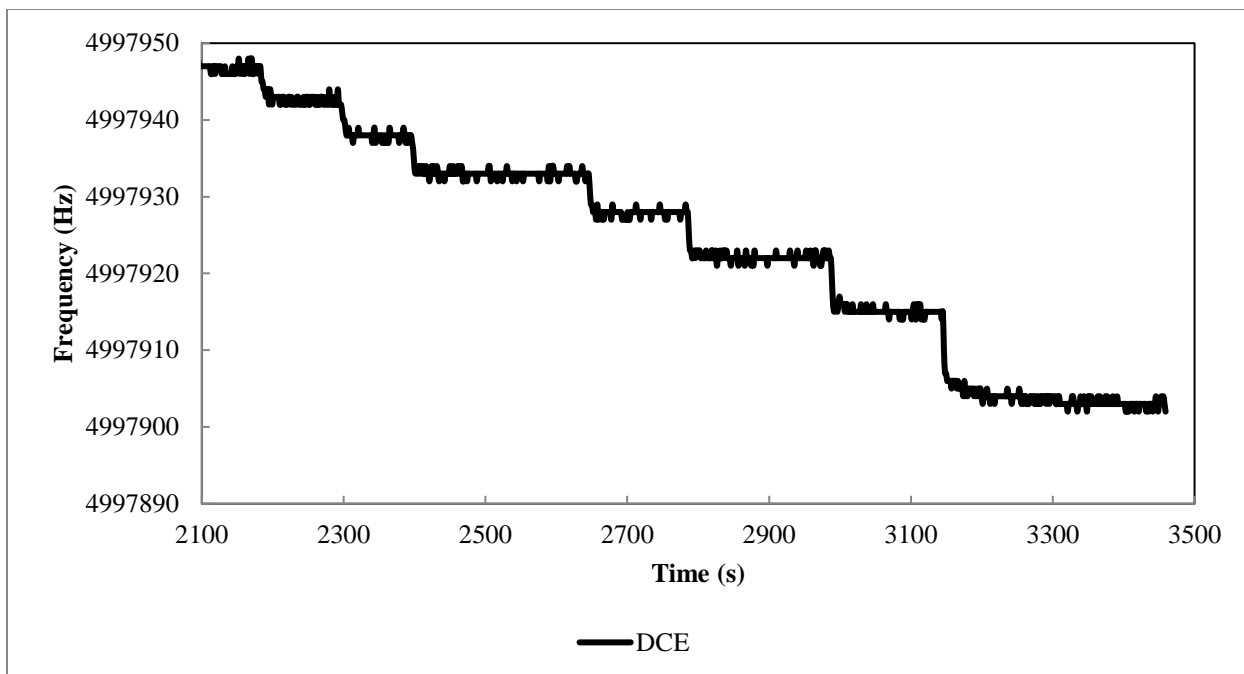Figure A.12 Frequency-time curve for sorption of DCM in PCL at 298.15 K

52

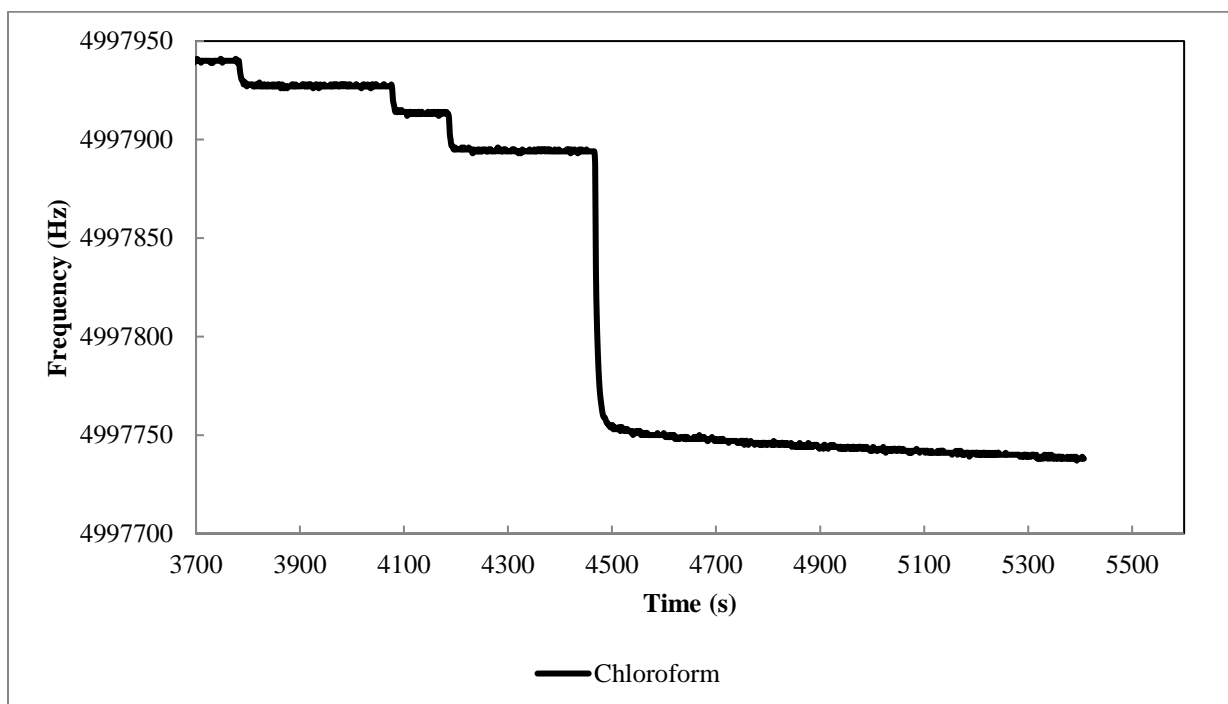Figure A.13 Frequency-time curve for sorption of DCE in PEG at 298.15 K

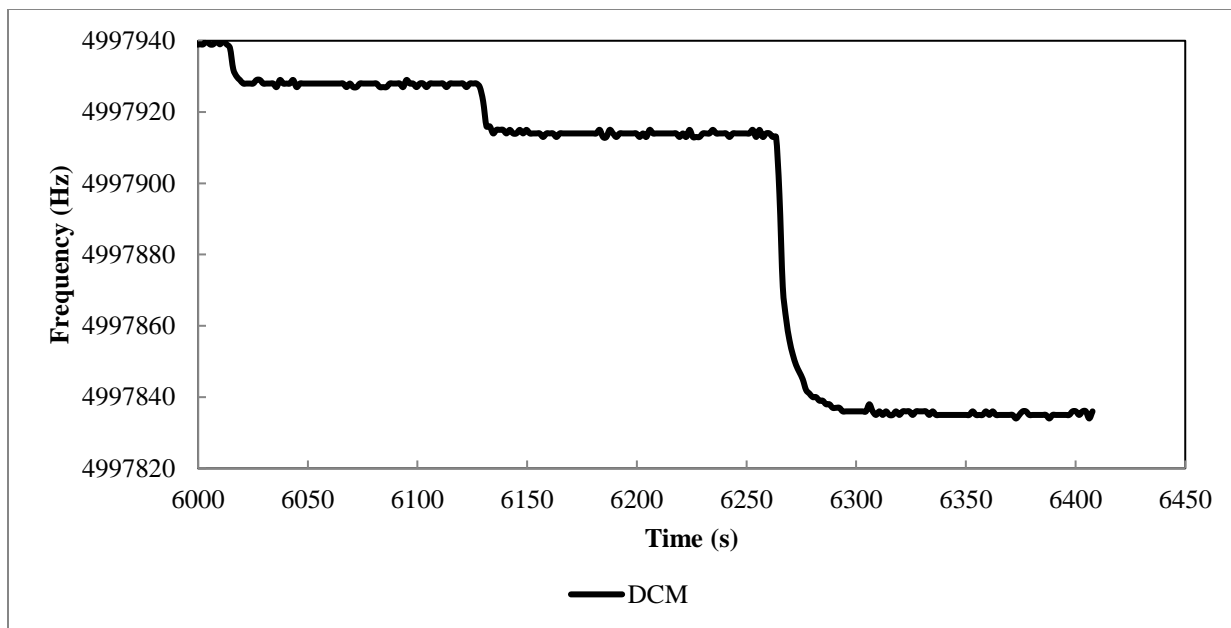Figure A.14 Frequency-time curve for sorption of chloroform in PEG at 298.15 K

Figure A.15 Frequency-time curve for sorption of DCM in PEG at 298.15 K